→ RESEARCH LIBRARY
key words: 1398
1- connections
2- seismic design

A PRELIMINARY STUDY ON ENERGY DISSIPATING CLADDING-TO-FRAME CONNECTIONS

by

Julie Mark Cohen — author

Director

Cladding Research Institute

6 Commodore Drive, Suite 330

Emeryville, CA 94608

Graham H. Powell

Professor

Department of Civil Engineering

University of California at Berkeley

Berkeley, CA 94720

A Report to Sponsors:

American Institute of Steel Construction

American Iron and Steel Institute

Nippon Steel Corporation

Report No. UCB/EERC-91/09

Earthquake Engineering Research Center

College of Engineering

University of California

Berkeley, California

September 1991

CLADDING RESEARCH INSTITUTE
6 Commodore Drive, Suite 330
Emeryville, California 94608 USA
(510) 654-7917
16 December 1991

Mr. Nestor R. Iwankiw, Director
Research and Codes
American Institute of Steel Construction, Inc.
One East Wacker Drive, Suite 3100
Chicago, Illinois 60601-2001

Dear Mr. Iwankiw:

Professor Graham H. Powell and I would like to thank you and AISC for your seed grant through U.C. Berkeley in support of our preliminary research dealing with structural steel cladding and energy dissipating cladding-to-frame connections. We are most appreciative for your support, because we could not have completed our study without your help.

Enclosed please find a preprint of our recently completed *Report No. EERC/UCB-91/09* entitled "A Preliminary Study on Energy Dissipating Cladding-to-Frame Connections." The report has been sent to the publisher and will be available in January 1992. Based on this report, we have submitted a paper entitled "A Preliminary Study on an Energy Dissipating Cladding System" to *Earthquake Engineering and Structural Dynamics* in which we have acknowledged AISC's sponsorship of our work.

Our studies suggest that the use of structural cladding and energy dissipating cladding-to-frame connections could be feasible for seismic retrofit and new construction. We hope to to continue our work if additional funding can be procured. We would be pleased if you would like contribute additional funds to our effort, and if you can put use in touch with specific companies that might be interested in becoming cosponsors. Please note that continuing studies will be conducted by me through the Cladding Research Institute. I am currently contacting San Francisco-Bay Area practitioners to procure as-built drawings of existing older (steel) framed buildings to use for topics that we have identified for further study.

Again, thank you very much. We shall look forward to hearing from you.

Sincerely,

Julie Mark Cohen

Julie Mark Cohen, Ph.D., P.E.
Director

Encl.
cc: G.H. Powell
Files

ABSTRACT

A preliminary study has been conducted to explore the use of structural cladding panels with energy dissipating cladding-to-frame connections for seismic resistant design. The study identifies several issues involved in the modelling and analysis of frames with energy dissipating cladding-to-frame connections, establishes concepts for design, and provides a preliminary assessment of the force and deformation demands that are likely to be placed on panels and connections.

Four hypothetical steel frames are considered in the study. An unclad reference frame is designed for 100% of the UBC [1991] strength and stiffness requirements, without any contributions from the cladding. This frame serves as a reference for making design decisions for the clad frames. For the first clad frame study, a bare steel frame is designed, but, due to construction errors, is found to provide only 66^2/3% of the required strength. The decision is made to retrofit the frame by using structural cladding and energy dissipating cladding-to-frame connections to provide additional strength and stiffness. For the second clad frame, a bare steel frame is designed to meet the strength requirements for 25% of the UBC [1991] loads, but not the drift requirements. Cladding is added to provide additional strength and stiffness. For the third clad frame, a bare frame is designed for gravity load only. Cladding is added to provide 100% of the lateral stiffness and strength.

Nonlinear dynamic analyses were performed to explore the effects of employing energy dissipating devices as cladding-to-frame connections. These analyses indicate that the clad frames perform well, based on observations about maximum interstory drifts, maximum plastic hinge rotations in the frames, and maximum ductility demands on the cladding-to-frame connections. In particular, story-to-story drifts are smaller than for the reference frame. Plastic hinge rotations in the frame members are correspondingly reduced. The ductility demands on the panel-to-frame connections are modest, and the forces transmitted to the cladding panels appear to be reasonable.

ACKNOWLEDGEMENTS

The research described in this report was completed under the co-sponsorship of the American Institute of Steel Construction (AISC), the American Iron and Steel Institute (AISI), and the Nippon Steel Corporation. The support from the following individuals is gratefully acknowledged: Mr. Nestor Iwankiw (Director of Research and Codes, AISC, Chicago), Mr. David C. Jeanes (Vice President, Market Development, AISI, Washington, D.C.), Ms. Kathleen H. Almand (Program Manager, AISI, Washington, D.C.), Mr. Yoshitaka Shibusawa (Nippon Steel Corporation, Los Angeles), and Mr. Yoshikazu Shinmi (General Manager, Construction and Architectural Materials, Development and Engineering Services Division, Nippon Steel Corporation).

Dr. Cohen wishes to thank Dr. Samuel J. Errera (retired, Bethlehem Steel, Bethlehem, PA) for his suggestion of the use of structural steel cladding, and for his continued support and encouragement while funding was being sought. Mr. Roger L. Brockenbrough (U.S. Steel, Monroeville, PA) is also thanked. Dr. Yousef Bozorgnia is thanked for his helpful discussions.

Assistance with DRAIN-2DX has been provided to Dr. Cohen by Vipul Prakash, Ph.D. candidate in SEMM, Department of Civil Engineering, University of California at Berkeley.

TABLE OF CONTENTS

TABLE OF CONTENTS (cont'd)

TABLE OF CONTENTS (cont'd)

LIST OF TABLES

LIST OF FIGURES

NOTATION

A	=	subscript that refers to Unclad and Clad Frames A
B	=	subscript that refers to Unclad and Clad Frames B
C	=	$(1.25S)/(T^{2/3})$, product that is a function of soil factor and fundamental period, used in the calculation of base shear V
$\underline{C}$	=	damping matrix
C_t	=	numerical coefficient for building frame frame used in calculation of base shear
C	=	subscript that refers to Unclad and Clad Frames C
D	=	Dead Load (psf)
E	=	elastic modulus of steel (ksi), or Earthquake Load (kips)
F_t	=	portion of the base shear considered concentrated at the top of the structure in addition to the lateral force applied at the Roof (kips)
h	=	or H, interstory building height (in.)
h_n	=	overall building height (ft.)
I	=	building importance factor used in calculation of base shear V
$\underline{K}_0$	=	stiffness matrix
K_1	=	or K1, initial stiffness of inelastic top panel connections at one floor (kip/in.)
k_1	=	or k1, initial stiffness of one top panel connection (kip/in.)
K_2	=	or K2, post-yield stiffness of inelastic top panel connections at one floor (kip/in.)
k_2	=	or k2, post-yield stiffness of one top panel connection (kip/in.)
K_2/K_1	=	or k_2/k_1, strain-hardening ratio
L	=	Live Load (psf)
LRFD	=	load and resistance factor design
M	=	moment (kip-in.)
$\underline{M}$	=	mass matrix
n	=	subscript that refers to "nominal". M_n = nominal moment capacity.
P_c	=	force in top inelastic connections for one floor (kips)
P_{max}	=	maximum force in top inelastic connections for one floor (kips)
P_y	=	yield strength of top inelastic connections for one floor (kips)
R_w	=	overstrength and ductility factor
R	=	subscript that refers to reference frame, Frame R
S	=	site coefficient for soil characteristics used in calculation of base shear V
T	=	or T_1, fundamental period (sec.)

NOTATION (cont'd)

u	=	displacement in global x direction
V	=	base shear (kips)
v	=	displacment in global y direction
W	=	building weight (kips)
Z	=	seismic zone factor used in calculation of base shear V
α	=	mass proportional damping factor
β	=	stiffness proportional damping factor
Δt	=	time integration step (sec.)
δ	=	interstory drift or deformation of top panel connection (in.)
δ_{max}	=	maximum deformation of inelastic top panel connection (in.)
δ_y	=	or Δ_y, yield deformation of inelastic top panel connection (in.)
δ/h	=	interstory drift ratio
ξ	=	critical viscous damping (%)
θ	=	rotation about glabal z axis (rad.)
μ	=	ductility ratio = δ_{max}/δ_y

CHAPTER 1

INTRODUCTION

1.1 Problem Statement

Since the introduction of the curtain wall in the late 1920s, cladding has usually been regarded as nonstructural. However, cladding *does* have a significant effect on the behavior of structures. Studies of response of tall buildings support this statement, because measured deflections tend to be smaller than computed deflections (see Miller [1972]). In addition, Henry and Roll [1986], Goodno and Palsson [1986], and PCI [1989] have shown that precast concrete cladding has a significant influence on the behavior of clad frames. Differences were found between clad and unclad frames for lateral displacement, natural frequency, and frame member force distribution. Significant forces were present in panel-to-frame connections. Davies and Bryan [1982] concluded that "stressed skin action is present whether the designer acknowledges it or not."

Since even "nonstructural" cladding has a significant effect on structural behavior, it is natural to ask whether performance under wind and seismic loads can be improved by explicitly utilizing the stiffness and strength of the cladding. The question is particularly pertinent for seismic performance, using energy dissipating cladding-to-frame connections to add damping, stiffness and ductility to buildings. There are possible applications in both new construction and seismic retrofit. In addition, there can be an increased flexibility in the use of interior space, because some or all of the interior lateral bracing can be omitted.

1.1.1 Practical Applications of the Stressed Skin Design Concept

As yet, there do not appear to have been any applications of structural cladding for seismic resistant design. However, the design of the fifty-four story One Mellon Center in Pittsburgh, PA, has helped to establish concepts and details for stressed skin steel cladding (Tomasetti, *et al.* [1986a,b], [1984]). They state that this design "represents the first development of a thin wall metal facade panel (stressed skin tube) to provide major stiffness in a high-rise building." Advantages included: a 50% reduction in deflections compared with the unclad frame; substantially smaller member sizes than would be needed for an unclad frame; a decrease of floor-to-floor height to 12 ft.; and an increase in usable floor space.

The stressed skin panels are 10 ft. wide and three stories (36 ft.) in height, with two window openings in each story. According to Tomasetti, *et al.* [1984], "The use of solid panels with only 25% glazing gives a visual weight similar to the surrounding traditional buildings, while aiding energy conservation." The panels consist of $^{1}/_{4}$ in. to $^{5}/_{16}$ in. thick A36 steel face plates, a grid of 4 in, 5 in., and 6 in. deep A36 stiffeners aligned with the window edges, and bent plates or angles at the panel edges. The weight per panel at the lowest floors is on the order of 7.2 to 8.1 kips, including insulation, glazing, nonstructural column covers, and connections welded to the panels. Hence, the average weight of the heaviest panels is approximately 21 to 22.5 psf.

The detailing of the panels was critical because they must act as shear diaphragms, yet be isolated from the effects of column shortening, especially during erection, and girder flexure (i.e., isolated against transfer of gravity load from the frame). The panel connections must thus be designed to transfer shear between panels and from the panels to the frame, but not to transfer vertical forces into the panels as the frame deforms under gravity loads. To satisfy these requirements, Tomasetti, *et al.*, used panel-to-frame connections consisting of vertical fins at panel mid-height, flexible horizontal plates at panel top and bottom, and flexible tiebacks at window heads and sills (see Fig. 1.1a).

The connections at the vertical panel edges provide for the transfer of vertical shear forces between panels and from the panels to the frame, while ensuring that column shortening due to gravity load is not transferred to the panels. For the connections at the interior of any building face, only small amounts of shear are transferred to the columns, and the main shear transfer is from panel-to-panel. At the end columns, all of the panel shear must be transferred to the columns. Hence, short connection fins are used for interior columns, and long and stronger ones for end columns. These connections are shown in Fig. 1.1b.

The primary horizontal connections are made at the top and bottom of the panels at every third floor, and are full length between columns. They have the following functions: the transfer of horizontal shear between upper and lower panels; the transfer of one floor of horizontal wind shear from the frame into the panels; and the relief of vertical stress in the panels due to frame shortening, spandrel beam flexure, and thermal effects. At the intermediate floors, horizontal connections transfer one floor of wind shear from the frame into the panels. They are slightly less than 2.5 ft. in length and are centered along the spandrel beam within the bay.

The tiebacks provide resistance against wind and normal pressures and hold the grid against buckling (see Fig. 1.1b).

1.1.2 Seismic Research on Cladding-to-Frame Connections

For seismic loads, only limited research-oriented studies have been conducted. Available results by Pinelli, *et al.* [1990a, 1990b] dealt with precast concrete cladding panels and cast-in-place steel inserts that were built-up from reinforcing bars welded to steel plates. The primary conclusion was that the inserts tend to work themselves loose. The researchers stated, "At low levels of load, stiffness (was) provided primarily by the concrete surrounding the insert. As the magnitude of the load cycles was increased, the concrete began to deteriorate. In many cases, the concrete failure was sudden and brittle... Once the concrete failed, the connections (became very flexible). Ultimately, the connection failed by a total collapse of the concrete or (by) failure of the weld between the steel plate and the rebar." The researchers planned to test additional inserts to help define an analytical nonlinear hysteretic model for cladding connections. They stated, "Such an improved representation will permit more accurate investigations of the effect of cladding on energy dissipation."

No other studies were found on either the development of better behaving inserts, or on the idea of using devices specifically designed as energy dissipators to connect the panels to the frame.

1.1.3 Needed Research

Before the concept of structural cladding and structural cladding-to-frame connections can be applied, many problems need to be solved, in both the architectural and structural engineering disciplines. There are four general problem areas. First, architectural studies are needed to determine when the use of structural cladding might be an appropriate design solution. Second, structural engineering studies are needed to determine when structural cladding with energy dissipating connections can be effective and efficient. Third, issues pertaining to the detailed structural behavior of the frame, stressed skin and connections need to be addressed. Fourth, methods for detailed structural design and analysis need to be developed.

In this study, issues involved in the design and analysis of frames with energy dissipating cladding-to-frame connections have been explored, and preliminary assessments have been made. The issues include:

(1) Design of the steel frame.
(2) Stiffnesses and yield strengths needed for both elastic and inelastic cladding-to-frame connections.
(3) Force and ductility demands on the cladding-to-frame connections. Some connections are designed to remain elastic and some to dissipate energy through inelastic action.
(4) Ductility demands for the members of the structural frame.
(5) Energy dissipated by the inelastic connections.
(6) Shear forces in the cladding panels.

1.2 Overview of Present Study

The building examined in this study is a steel-framed structure, three bays by five bays in plan and five stories in height. Simple interior framing is assumed, with all lateral resistance provided by the perimeter frame. Since UBC [1991], AISC [1990] and SEAONC [1990] do not contain criteria for the design of framing systems with energy dissipating cladding-to-frame connections, three different design scenarios were assumed. These are as follows:

(1) Scenario 1: A bare steel frame is designed as a special moment-resisting frame (SMRF) to meet strength requirements for 100% of the UBC [1991] loads. However, construction deficiencies are found in the girder-column connections that result in non-ductile connections, and the building was found to be excessively flexible. The decision is made to retrofit the building by using structural cladding and energy dissipating cladding-to-frame connections. For the retrofit design, the frame is treated as an ordinary moment-resisting frame (OMRF) for which the cladding and connections provide additional strength and stiffness. This is Building A.

(2) Scenario 2: A bare steel frame is designed to meet the strength requirements for 25% of the UBC [1991] loads, but not the drift requirements. Cladding is added to provide additional strength and stiffness. This is similar to the "dual system" provisions in the UBC [1991]. This is Building B.

(3) Scenario 3: A bare frame is designed for gravity load only. Cladding is added to provide 100% of the lateral stiffness and strength. This is Building C.

For each building, the unclad frame is first designed, based on the pseudo-static method from UBC [1991], AISC LRFD [1986], and AISC [1990]. Structural cladding and cladding-to-frame connections are then added to satisfy additional strength and stiffness criteria. The practical example cited in Section 1.1.1 was used as a basis for design decisions for the cladding and connections. From this, an effective panel thickness, and weight were assumed. Also from this example, assumptions were made for the panel-to-frame and panel-to-panel connection designs, including the locations of the connections and the types of force transmitted.

Inelastic dynamic analyses were then performed to investigate the force, deformation, and ductility demands on the frame members, panels and connections.

1.3 Report Contents

Chapter 2 contains a description of the building selection and design. The modelling for analysis is described in Chapter 3. In Chapter 4, the analysis results and summary are presented. The conclusions from the preliminary study, and an outline of topics for further study are given in Chapter 5.

CHAPTER 2

BUILDING SELECTION AND DESIGN

2.1 Description of Building

A low-rise building with regular geometry and framing was chosen as the basis for the preliminary study. Specifically, a five story steel-framed (office) building with a perimeter frame system, three-by-five bays in plan, was chosen. The frames analyzed in the study are the three-bay wide exterior frames. The first floor was assumed to be the same height as the upper floors. All bays on the building perimeter were assumed to be clad.

2.2 Design Concept and Assumptions

2.2.1 Floor Framing

A cast-in-place reinforced concrete floor slab with steel beams and girders was assumed. The framing plan of a typical floor is shown in Fig. 2.1. The beams are oriented along the long axis of the building, and frame into transverse girders. The gravity loads were thus supported by the interior and exterior structural steel frames in the three-bay direction.

2.2.2 Structural Steel Frames

The lateral force resisting concept chosen for the structural frame is perimeter frame lateral resistance. For this concept, the interior beam-column connections are simple connections, and the girder-to-column connections along the perimeter of the building are moment-resisting. The exterior moment-resisting frames analyzed for this study are in the short direction. These frames are designed for gravity loads, including cladding weight, and seismic lateral loads including, cladding mass. All floor-to-floor heights are 12 ft. (see Fig. 2.2). The column bases are assumed to be fixed.

For conventional moment-resisting frames that provide the only source of lateral resistance for seismic loads, the ideal inelastic behavior is uniform energy dissipation in the girders at all floors in all bays, with strong column-weak beam behavior. This helps ensure that excessive interstory drifts do not occur. To accomplish this, the girders in each bay at each floor should yield essentially uniformly, and subsequent inelastic deformations should keep the interstory drifts within prescribed limits.

For a frame with structural cladding and energy dissipating connections, the ideal inelastic behavior is analogous to this. However, the primary source of energy dissipation is in the cladding-to-frame connections, rather than in the girders. The inelastic connections should be designed to yield essentially uniformly, with inelastic deformations that keep interstory drifts within prescribed limits.

One design criterion is thus to have all of the connections yield at approximately the same time. A second criterion is to limit the ductility demands so the interstory drifts are not excessive.

2.3. Unclad Frame Design Procedure

2.3.1 General

In addition to the frames for Buildings A, B, and C, a reference frame, Frame R, was also designed. Frame R is designed for 100% of the UBC [1991] strength and stiffness requirements, without any contributions from the cladding. It serves as a reference for making design decisions for the clad frames.

The design procedures for the unclad frames are described in Sections 2.3.2-2.3.5. The design procedure for the cladding is described later.

2.3.2 Reference Frame (Frame R)

Frame R is designed for $R_w = 8$ and 100% of the strength and stiffness requirements. The design procedure followed UBC [1991] and included the following:

(1) The first mode period, $T = C_t(h_n)^{3/4}$, was calculated as 0.755 second.

(2) The base shear, $V = (ZIC/R_w)W$, was calculated as 0.0754W, where $Z = 0.4$ for Zone 4, the importance factor $I = 1.0$, and $C = (1.25S)/(T^{2/3}) = 1.508$ for a soil factor of $S = 1.0$.

(3) The portion of the base shear considered concentrated at the top of the structure, F_t, was calculated as 0.07TV. Hence, $F_t = 0.0053V$.

(4) The vertical distribution of lateral loads was then calculated. These loads are given in Table 2.1.

(5) The frame was designed for gravity loads (1.2D + 1.6L), and combined gravity and lateral loads (1.2D + 0.5L + 1.5E) per equation (2-5) in AISC [1990], based on a linear elastic static analysis. The dead and live gravity loads, D and L, are given in Fig. 2.1.

(6) The strong column-weak beam concept was imposed.

(7) Frame members were designed so that the drift for the lateral loads, 1.0E (see Table 2.1), did not exceed the drift limit of $(0.03/R_w)h$ in any story, where h = story height. This limit is 0.00375h = 0.54 in.

The member sizes for Frame R are given in Fig. 2.2.

2.3.3 Unclad Frame A

For this scenario, the original design provided 100% of the lateral resistance with $R_w = 12$. The drift limit at 1.0E for this frame is $0.03/R_w = 0.0025H$. This frame is labelled Unclad Frame A. The unfactored lateral loads, $1.0E_A$, are given in Table 2.1. The member sizes are given in Fig. 2.2.

Construction deficiencies were found in the girder-column connections, and the building was found to be excessively flexible. As a result, the as-built frames were re-classified to be slightly better than ordinary moment-resisting frames (OMRF) with $R_w = 8$ (instead of $R_w = 6$), and the decision was made to retrofit the frames with structural cladding and energy dissipating cladding-to-frame connections. To achieve a design for $R_w = 8$, the frame provides $66^2/3$% of the lateral strength (since it was designed for $R_w = 12$), and the cladding panels and connections must provide additional stiffness and $33^1/3$% of the lateral strength. Since the girder-column connections are not ductile, the inelastic cladding-to-frame connections should be considered as the primary source of energy dissipation

2.3.4 Unclad Frame B

In this scenario, this is a design for which 25% of the lateral resistance is provided by the two bare exterior frames with $R_w = 8$. Since $R_w = 12$ is used for steel frames with ductile detailing, a smaller value of R_w was judged to be more appropriate for this type of frame, where the primary source of ductility is found in the inelastic cladding-to-frame connections.

The design loading for combined gravity and lateral load was $1.2D + 0.5L + 1.5E_B$, where E_B is equal to 25% of the lateral loads for Frame R, or $0.25E_R$. The strong column-weak beam concept was imposed. This is labelled Unclad Frame B. The loads, $1.0E_B$, are given in Table 2.1. The member sizes are shown in Fig. 2.2.

The cladding panels and connections provide additional stiffness and 75% of the lateral strength. It is desirable that the cladding-to-frame connections provide the primary source of energy dissipation.

2.3.5 Unclad Frame C

No lateral resistance is provided by either of the two bare frames, and the girder-column connections are non-moment-resisting. The design gravity loads, including cladding weight, were $1.2D + 1.6L$. Lateral strength and stiffness were not design criteria. This frame is labelled Unclad Frame C. The lateral loads, $1.0E_C$, are equal to the lateral loads for Frame R, $1.0E_R$, and are given in Table 2.1. The member sizes are given in Fig. 2.2.

The cladding panels and connections provide 100% of the lateral strength and stiffness, with $R_w = 8$. The cladding-to-frame connections provide the sole source of energy dissipation.

2.4 Design Assumptions for Cladding Panels and Connections

The weight of each 24 ft. wide and 12 ft. tall panel with insulation and sub-framing is assumed to be 10 kips, or 35 psf. As noted in Section 1.1.1, for the One Mellon Center building the panels weigh about 22.5 psf. However, the panels in the current building need to be stronger to resist seismic forces. Accordingly, a weight of 35 psf has been assumed, which includes thicker stiffeners and additional sub-framing members for the panels. The effective shear stiffness is based on a panel thickness of $^9/16$ in. As a consequence, the panels are very stiff and are assumed to be elastic and virtually rigid. The panels account for 14% of the total building mass.

The panels are attached to the frame as shown in Figs. 2.3a and 2.3b. The connections support the weight of the panels and transmit shear forces from the frame to the panels. The connections do not transmit compression forces to the panels from column shortening, beam flexure, or thermal movement. Details are as follows:

(1) Horizontal shears are transferred between the spandrel beams and panels through the connections along the horizontal bottom and top edges of the panels (see Figs. 2.3a and 2.3b). At the bottom edges of the panels, the connections are designed to be elastic. At the top edges of the panels, the connections are designed to be inelastic, and hence energy dissipating. These connections remain elastic for wind loads and mild earthquakes. The bottom and top connections are flexible in the vertical direction. This flexibility eliminates compression forces in the panels from column shortening, beam flexure, and differential thermal movement. The connections are assumed to have no rotational stiffness.

(2) Vertical shear is transferred between the columns and panels through the connections along the vertical edges of the panels (see Figs. 2.3a and 2.3b). The connections are attached at mid-height of the columns. They also support the gravity load of the cladding. These connections are short and fin-like, so that column shortening and differential thermal movement do not compress the panel. The connections are designed to remain elastic. They are flexible in the horizontal direction and have no rotational stiffness.

(3) At each horizontal edge, separate connections are assumed for the panels in the stories above and below (i.e., an elastic connection for the panel above, and an inelastic connection for the panel below). There is no direct panel-to-panel connection. It is noted that in the One Mellon Center, the panels were directly connected in three bay tiers. This type of configuration has not been explored in the current study.

(4) At each vertical edge, a single elastic "fin" connection is assumed, connected to both the left panel and the right panel. This provides for force transfer from panel to column and also directly from panel to panel (see Fig. 2.3b).

2.5 Design Procedure for Inelastic Connections

2.5.1 General

For the inelastic connections, initial stiffnesses, yield displacements, yield strengths, and strain-hardening ratios need to be chosen. The choices of connection stiffness and yield strength are a critical aspect of the design process. These values must provide satisfactory building performance and also be within a practical range for actual hysteretic yielding connection devices.

2.5.2 Connection Strengths

The frame provides some of the lateral strength, and the panels and connections provide the rest. The design lateral loads for the clad frames are $1.5E_R$, where R refers to the Reference Frame R. For Clad Frame A, the frame resists $66^2/3\%$ of this load, while the cladding panels and connections resist the remaining $33^1/3\%$. For Clad Frame B, the frame resists 25%, and the cladding panels and connections resist the remaining 75%. For Clad Frame C, the frame resists no lateral loads, and the cladding panels and connections provide 100% of the lateral resistance. To satisfy these criteria, it is necessary to choose the connec-tion strengths.

The required connection strength at any story is equal to the story shear that must be resisted by the panels and connections at each story. Since there are three connections per floor, the strength of each connection is equal to one-third of the required strength at each story.

The story shears to be resisted by the panels and connections can be based on either nominal strengths or on more realistic actual strengths. Consider Clad Frame B as an example. The nominal story strengths of Unclad Frame B are equal to the story shears due to lateral loads $(0.25)(1.5E_R) = 0.375E_R$. The nominal strengths to be provided by the connections are thus the story shears due to $(0.75)(1.5E_R) = 1.125E_R$. If the actual strength of the unclad frame is equal to the nominal strength, then with this design procedure the nominal and actual strengths of Clad Frame B will be $1.5E_R$, equal to that of Frame R.

However, the actual strength of Unclad Frame B is not $0.375E_R$, but is substantially larger than this value.[1] The reason for this is that the strength limit state for frame design is essentially formation of the first plastic hinge. Since all members are not fully stressed at this limit state, substantial additional lateral load can be resisted before a collapse mechanism develops. To determine the actual strength, a static lateral push-over analysis was performed for loads $1.2D + 0.5L + xE$, to determine the value of x at collapse. For this analysis, plastic hinges with zero strain-hardening were allowed to form at the member ends. The hinge strengths were equal to the factored nominal member moment capacities, ϕM_n (see AISC [1986]). The value of x was determined as 2.38 times the nominal strength, or $(2.38)(0.375E_R) = 0.893E_R$. The "overstrength" of Unclad Frame B is thus 138%. This does not mean, however, that the connections can be weaker. The reason is that the actual strength of Frame R is also larger than its nominal strength. For Frame R, the overstrength was determined as 70%, again by static push-over analysis. To be consistent, Clad Frames A, B, and C each should have an actual strength comparable to Frame R.

In order to obtain a strength equal to that of Frame R, the connections in Clad Frame B must

---

1 Some of the sources of overstrength include: member oversizing due to stiffness (drift) requirements, an increase in lateral strength from gravity effects on combined gravity and lateral load design, differences between design force demands and member strengths due to discrete choices of member sizes, code minimum requirements for strength, and redistribution of internal forces in the inelastic range.

be designed for the difference between the actual strength of Frame R and the actual strength of Unclad Frame B, or $(1.70)(1.5E_R) - (2.38)(0.25)(1.5E_R) = 1.66E_R$. Similar calculations can be performed for Clad Frames A and C. The connection design loads resulting from these calculations are shown in Fig. 2.4a for nominal strengths and Fig. 2.4b for actual strengths.

In Fig. 2.4a, the left-most bar represents the nominal strength of Frame R. Nominal strength is also referred to as 0% overstrength. In each of the three bars to the right, for Clad Frames A, B, and C, the sum of the unclad frame strength plus the connection strength equals the nominal strength of Frame R. The required connection strengths are equal to the story shears to be resisted by the connections. These strengths are given in Tables 2.2a and 2.2b.

In Fig. 2.4b, the left-most bar represents the actual strength of Frame R, which includes the nominal strength plus the overstrength of 70%. In the three bars to the right, for Clad Frames A, B, and C, the sum of the unclad frame strength plus the connection strength equals the actual strength of Frame R. For Unclad Frames A and B, the actual strengths are 66% and 138% larger than the nominal strengths. For Clad Frame A, the frame contributes 65% of the strength and the connections contribute 35%. For Clad Frame B, the frame contributes 35% of the strength and the connections contribute 65%. For Clad Frame C, the frame contributes 0% of the strength and the connections contribute 100%. As can be seen from a comparison of Figs. 2.4b and 2.4a, the connections need to be stronger for the 70% overstrength design. The values of the required connection strength are given in Tables 2.3a and 2.3b.

2.5.3 Connection Yield Displacements and Stiffnesses

It is also necessary to choose the initial stiffnesses of the connections (i.e., stiffness before the connections yield). These stiffnesses are based on drift considerations, as follows.

The horizontal displacements of the top panel connections are approximately equal to the interstory drifts of the frame, because the panels remain essentially rigid, and because the side and bottom connections for each panel are assumed to be very stiff. Therefore, the drift limits for the frame can be used to determine the yield displacements of the inelastic connections.

For the 0% overstrength design, the connection stiffnesses were determined by assuming that the connections yield at the nominal strength $1.5E_R$ and at a drift of 0.00375h. This was rather an arbitrary decision. An alternative was to satisfy the drift serviceability limit of 0.00375h at $1.0E_R$, but is is believed that a stiffer design is desirable.

For the 70% overstrength design, there are two options as follows:

Option 1: Use the same connection stiffnesses as for the 0% overstrength design. This gives the same frame stiffness before yield of the connections, but since the connections are stronger the drift at connection yield is larger than 0.00375h.

Option 2: Use the same connection yield deformation as for the 0% overstrength design.

This gives a larger stiffness for the frame before the connections yield, and the connections yield at a drift of 0.00375h.

These two options are illustrated in Figs. 2.5a, 2.5b, and 2.5c. The connection stiffnesses for the 0% and 70% overstrength designs are given in Tables 2.2c, 2.3c, and 2.4b.

2.5.3.1 Strain-Hardening Ratios

The connection strain-hardening ratio is also an important parameter. This is the post-yield stiffness divided by the initial stiffness, k_2/k_1 (see Fig. 2.5a). Experimental and theoretical studies of inelastic seismic response have tended to show that large drifts may occur if the effective strain-hardening ratio of a structure is zero. This observation could particularly apply to Clad Frame C, because the frame has no lateral stiffness, and hence contributes no effective strain-hardening.

For the preliminary study, two strain-hardening ratios, $k_2/k_1 = 0.0$ and 0.1, have been assumed. The value $k_2/k_1 = 0.0$ might represent a friction-damping device without a restoring spring. The value $k_2/k_1 = 0.1$ might represent a metallic yielding device or a friction-damping device with restoring springs.

2.5.4 Summary of Connection Design Concept

The connection design concept includes combinations of two strength levels, and two yield deformation levels as follows:

2.5.4.1 Concept I

The connection yield strengths, P_y, are based on 0% overstrength of Frame R (see Tables 2.2a and 2.2b). The yield displacements, δ_y, are specified as 0.00375h = 0.54 in. The stiffnesses, K_1, are calculated as P_y/δ_y for each floor. The values of K_1 are given in Table 2.2c. The stiffness of the connection in each bay is $k_1 = K_1/3$.

2.5.4.2 Concept II

The connection yield strengths, P_y, are based on 70% overstrength of Frame R (see Tables 2.3a and 2.3b). The stiffnesses, K_1, are the same as for Concept I. The yield deformations δ_y are equal to P_y/K_1. The yield deformations divided by story height are given in Table 2.3c.

2.5.4.3 Concept III

The connection yield strengths, P_y, are based on 70% overstrength of Frame R (see Tables 2.3a, 2.3b and 2.4a). The stiffnesses K_1 are increased so that the yield displacements, δ_y, are 0.00375h = 0.54 in. for this strength level. The values of K_1 are given in Table 2.4b.

Plots of connection strengths, P, versus connection displacement, δ, are shown for Concepts I, II, and III in Figs. 2.5a, 2.5b, and 2.5c. The relative magnitudes of strengths and stiffnesses for the three concepts are shown (also see Tables 2.2b, 2.2c, 2.3b, 2.3c, and 2.4b). The initial stiffnesses of the top panel connections for Concepts I and II are equal, and are less stiff than for Concept III. The yield strengths of the connections for Concepts II and III are equal, and are larger than for Concept I.

For each design concept, two strain-hardening ratios, $K_2/K_1 = 0.0$ and 0.1, were assigned. These values are rough lower and upper bounds for actual yielding devices.

In summary, there are three clad frames; for each clad frame there are three design concepts for the inelastic connections, Concepts I, II, and III; and for each concept there are two strain-hardening ratios. In total, there are eighteen different cases.

2.6 Design Procedure for Side and Bottom Connections

The side panel connections are short and fin-like. The stiffness used in the preliminary study was assumed to be 1000 kip/in. The connections were assumed to be infinitely strong.

Bottom panel connections were assumed to extend over the full bay width, as in the One Mellon Center building. The stiffness used in the preliminary study was assumed to be 1.5×10^6 kip/in. The connections were assumed to be infinitely strong.

CHAPTER 3

MODELLING FOR ANALYSIS

3.1 Overview

The analyses entailed modelling the cladding and the cladding-to-frame connections, and choosing the appropriate ground motions. Described in this section are the computer program used, the nonlinear model, the input ground motion, and the types of results obtained.

3.2 Computer Program

The analyses were performed using DRAIN-2DX. Allahabadi and Powell [1988] have summarized the features of DRAIN-2DX as follows:

"DRAIN-2DX is a computer program for the analysis of inelastic two-dimensional structures under static and dynamic loading, with particular emphasis on seismic response... DRAIN-2DX seeks to correct (the simplicity and lack of many desirable features in the original program, DRAIN-2D), by providing the following capabilities:

(1) "Nonlinear static, as well as dynamic, analyses can be performed.

(2) "More sophisticated dynamic step-by-step solution strategies may be specified. In particular, (a) the time step can be varied automatically (this is valuable for analyses involving gap closure), and (b) corrections can be applied to compensate for errors in force equilibrium and energy balance.

(3) "Energy balance computation can be performed, and detailed logs of energy and equilibrium error can be obtained.

(4) "Static and dynamic loads can be applied in any sequence.

(5) "The structure state can be saved permanently at the end of any analyses. A new analysis can then begin from any previously saved state.

(6) "Dynamic analyses can be carried out for ground accelerations (all supports moving in phase), ground displacements (supports may move out-of-phase), specified external forces (e.g., wind), and initial velocities (corresponding to an initial impulse).

(7) "Mode shapes and frequencies can be calculated, and linear response spectrum analyses can be performed.

(8) "Cross sections can be specified through a structure, and the resultant normal, shear and overturning effects on these sections can be computed."

The reader is referred to Allahabadi and Powell [1988] and Powell [1990] for additional information.

3.3 Modelling

3.3.1 Structural Elements

The frame, panels, and connections are modelled as a 2D structure. The frame consists of girders and columns, both of which are modelled as beam-column elements possessing flexural and axial stiffness. Centerline dimensions are used for the girders and columns; girder-column joints occur at column centerlines. Plastic hinges can occur at the girder and column ends. For both girders and columns, plastic hinge formation was assumed to be affected by bending only, ignoring the axial force effects. A strain-hardening stiffness of 2% was assumed. In Frame C, the girder ends are released to model simply supported girders. Each panel is modelled as a single structural element for which overall extensional, flexural, and shear stiffnesses are specified. The panels remain elastic. The connections are modelled as zero-length elements with bilinear behavior.

3.3.2 Viscous Damping

DRAIN-2DX allows for viscous damping, where the damping matrix, $\underline{C}$, is given by,

$$\underline{C} = \alpha \underline{M} + \beta \underline{K}_0$$

where $\underline{M}$ = the mass matrix and $\underline{K}_0$ = the initial elastic stiffness matrix, and α and β are mass and stiffness proportional damping factors. These factors can be chosen to provide specified proportions of critical damping at two selected periods, if both α and β are specified, or at one period if only α or β is specified (see Clough and Penzien [1975]).

Viscous damping of 2% of critical was assumed to be provided by the frame, panels, and connections at a period of 1 second, using only β. The value of α was set to zero. The value of β is equal to 0.0064.

Viscous damping allows for "miscellaneous" energy losses not accounted for directly in the inelastic model. Hysteretic damping provided by the inelastic cladding-to-frame connections is expected to account for the majority of energy dissipation.

To assess effects of viscous damping, one additional case was examined with viscous damping of 4%. For this, the value of β is 0.0127.

3.3.3 Constraints and Restraints of Nodes

The nodes used in modelling the clad frames are shown in Fig. 3.1. In DRAIN-2DX, the panel elements have nodes only at their corners. Since the panels connect to the frame at mid-length along the panel edges, additional nodes were needed to model the connections. The node locations are as follows:

(1) intersections of the girders and columns (Nodes 1, 3, 14, and 16),

(2) mid-height of the columns (Nodes 7 and 10),

(3) mid-length of the girders (Nodes 2 and 15), and

(4) corners of the panels (Nodes 4, 6, 11, and 13).

The frame Nodes 1-3, 7, 10, and 14-16 are not constrained or restrained. The nodes at the bottom of the columns at the 1st Floor are restrained against translation and rotation.

The cladding-to-frame connections are defined by four additional nodes that are not physically connected to either the panels or the frame. These are Nodes 5, 8, 9, and 12. They are constrained to the panel nodes as described below.

(1) The constraints in the horizontal direction are shown at the top of Fig. 3.1. The horizontal displacements of Nodes 4, 5, and 6 at the top of the panel are constrained to be equal; and the horizontal displacements of Nodes 11, 12, and 13 are constrained to be equal. These constraints apply to each panel individually. Nodes 8 and 9 are restrained horizontally, since the horizontal stiffnesses of the cladding-to-frame connections between Nodes 7 and 8, and 9 and 10 are zero.

(2) The nodes constrained in the vertical direction are shown at the bottom of Fig. 3.1. At the building exterior, the vertical displacements of Nodes 4, 8, and 11 at the left side of the panel are constrained to be equal. At the building interior, the vertical displacements of Nodes 6, 9, and 13 at the right side of the panel and the corner nodes at the left edge of the panel from the adjacent bay to the right (not shown in the figure) are constrained to be equal. Nodes 5 and 12 are restrained vertically, since the vertical stiffnesses of the cladding-to-frame connections between Nodes 2 and 5, and 12 and 15 are zero.

(3) Nodes 5, 8, 9, and 12 are all restrained against rotation, since the rotational stiffnesses of the cladding-to-frame connections between Nodes 2 and 5, 7 and 8, 9 and 10, and 12 and 15 are zero.

(4) Panel corner Nodes 4, 6, 11, and 13 are restrained against rotation.

3.4 Ground Motion

For the preliminary analyses, the S00E component of the 1940 El Centro earthquake, with a Richter magnitude of 6.7, was chosen. The component has a peak ground acceleration of 0.34g, and a predominant frequency range of 1-4 Hz. The first 15 seconds of the record were used, since preliminary analyses showed that, in some cases, the maximum value of forces and deformations occurred at approximately 12.4 seconds. The time step for step-by-step integration was chosen to be 0.01 second, with consideration of events within time steps.

During ground motion excitation, gravity loads equal to 1.0D + 0.5L were present.

One additional case was examined with a 0.005 second time integration step. No significant differences were found in the results obtained using this smaller time step.

3.5 Types of Results Obtained

For Frame R, the results obtained include the following:

(1) a more accurate value of the fundamental period than the value obtained from the approximation given in UBC [1991];

(2) maximum interstory drifts and maximum interstory drift ratios; and

(3) maximum plastic hinge rotations at the girder and column ends.

For Clad Frames A, B, and C, the results obtained include:

(1) fundamental periods;

(2) maximum interstory drifts and maximum interstory drift ratios;

(3) maximum plastic hinge rotations at the girder and column ends; and

(4) maximum deformations and ductility ratios of inelastic top panel connections.

In addition, the maximum forces in the elastic side panel connections, and the maximum shear forces in the panels were noted. However, no attempts were made to assess the adequacy of these connections or the panels.

CHAPTER 4

ANALYSIS RESULTS

4.1 Frame R

The fundamental period of Frame R was determined by a linear eigenvalue analysis. The maximum interstory drifts and interstory drift ratios, and plastic hinge rotations in the frame were determined by performing nonlinear dynamic analyses using DRAIN-2DX. The envelope values of the calculated response quantities are the larger of the maximum positive and negative quantities, unless otherwise noted. The maximum values are labelled as "envelope" values in the tables and figures.

4.1.1 Fundamental Period

The fundamental period for Frame R was calculated as 0.991 second (see Table 4.1). As noted in Section 2.3.2 on the design of Frame R, the fundamental period was determined to be 0.755 second from the approximate equation in UBC [1991].

4.1.2 Maximum Interstory Drifts and Maximum Interstory Drift Ratios

The maximum positive and negative interstory drifts and interstory drift ratios, along with their times occurrence, are given in Table 4.2. The largest interstory drift ratio is 1.57%. The maximum positive drifts occur within 0.29 second of each other; the negative drifts occur within 0.11 second of each other. This suggests that the first mode response dominates the behavior. The interstory drifts are larger in the upper stories, and the positive drifts are larger than the negative drifts.

4.1.3 Maximum Plastic Hinge Rotations in Frame

The maximum plastic hinge rotations are given in Table 4.7. The largest plastic hinge rotation is 0.0124 radian. The rotations at the Roof and 5th Floor are significantly larger than for the lower floors, as was observed for the interstory drifts. No plastic hinge rotations of any significance occurred at the bases of the columns.

4.2 Clad Frames A, B, and C

The fundamental periods of Clad Frames A, B, and C were determined by eigenvalue analyses. Maximum values of the following response quantities were determined by performing inelastic dynamic analyses: interstory drifts, interstory drift ratios, plastic hinge rotations, and deformations of the inelastic top panel connections, and ductility ratios for these connections. The maximum values are labelled as "envelope" values in the tables and figures. The envelope values are the larger of the maximum positive and negative quantities.

4.2.1 Fundamental Periods

The fundamental periods for Clad Frames A, B, and C are given in Table 4.1. The fundamental periods for the clad frames using design Concepts I and II for the top panel connections are approximately the same for all three frames, ranging from 1.211 to 1.293 second. The fundamental periods for the clad frames using design Concept III are smaller, ranging from 0.987 to 1.132 second. The fundamental period of Clad Frame C designed with connection Concept III at 0.987 second is the closest to the fundamental period of Frame R at 0.991 second.

4.2.2 Maximum Interstory Drifts and Maximum Interstory Drift Ratios

For Clad Frames A, B, and C, the envelopes of interstory drifts and interstory drift ratios, as well as the times of their occurrence, are given in Tables 4.3, 4.4 and 4.5, and 4.6, respectively. Uniformity of interstory drifts is desirable.

For Clad Frame A (see Table 4.3), some observations are as follows:

(1) All of the interstory drift ratios are substantially smaller than for Frame R. The maximum value is 1.32% for Concept I with $k_2/k_1 = 0.0$.

(1a) For Concept II, the maximum value is 1.30% with $k_2/k_1 = 0.0$; for Concept III, the maximum value is 0.92% with both $k_2/k_1 = 0.0$ and $k_2/k_1 = 0.1$.

(2) The maximum interstory drifts occur at different times during the response, suggesting significant contributions from higher modes.

(3) For connections with $k_2/k_1 = 0.0$ and $k_2/k_1 = 0.1$, the maximum interstory drift ratios occur within 0.01 second of each other, with only one exception. This indicates that the strain-hardening does not significantly change the dynamic properties.

(4) For the frames designed using connection Concepts I, II and III (with one exception for Concept III), the introduction of 10% strain-hardening (i.e., $k_2/k_1 = 0.1$) does not significantly decrease the interstory drift ratios. This aspect is considered further in Section 4.3.

For Clad Frame B (see Table 4.4), some observations are as follows:

(1) All of the interstory drift ratios are substantially smaller than for Frame R. The maximum value is 1.19% for Concept I with $k_2/k_1 = 0.0$.

(1a) For Concept II, the maximum value is 1.19% with $k_2/k_1 = 0.0$; for Concept III, the maximum value is 0.91% with $k_2/k_1 = 0.0$.

(2) The maximum interstory drifts occur at different times during the response, suggesting significant contributions from higher modes.

(3) For connections with $k_2/k_1 = 0.0$ and $k_2/k_1 = 0.1$, the maximum interstory drift ratios occur within 0.01 second of each other, with two exceptions. This indicates that the strain-hardening does not significantly change the dynamic properties.

(4) For the frames designed using connection Concepts I and II, the introduction of 10% strain-hardening (i.e., $k_2/k_1 = 0.1$) does not significantly decrease the interstory drift ratios in either the positive or negative directions. For the frames designed using connection Concept III, the introduction of 10% strain-hardening slightly decreases the interstory drifts between the 2nd and 5th Floors.

For Clad Frame C (see Table 4.6), some observations are as follows:

(1) The maximum interstory drifts for Concept I are larger than for Frame R. The maximum value, 1.58%, occurs at the top floor for Concept I with $k_2/k_1 = 0.0$. For the same frame, the maximum value at the ground floor is 1.46%.

(1a) For Concepts II and III, the interstory drift ratios are substantially smaller than for Frame R. For Concept II, the maximum value is 1.46% with $k_2/k_1 = 0.0$; for Concept III, the maximum value is 0.99% with $k_2/k_1 = 0.0$ and $k_2/k_1 = 0.1$.

(2) The maximum interstory drifts occur at different times during the response, suggesting significant contributions from higher modes.

(3) For connections with $k_2/k_1 = 0.0$ and $k_2/k_1 = 0.1$, the maximum negative interstory drift ratios occur within 0.09 second of each other, with only two exceptions. This indicates that the strain-hardening does not significantly change the dynamic properties in the negative direction. In the positive direction, however, almost all of the maximum interstory drift ratios occur at times that differ by 2 to 13 seconds.

(4) For the frames designed using connection Concepts I, II and III (with one exception for Concept III), the introduction of 10% strain-hardening (i.e., $k_2/k_1 = 0.1$) does not significantly decrease the interstory drift ratios in the positive direction. In the negative direction, almost all of the maximum interstory drifts were reduced by the introduction of 10% strain-hardening.

4.2.2.1 Time Step and Energy

For Clad Frame B designed using connection Concept III with 10% strain-hardening, the effects of two parameters on the interstory drifts are given in Table 4.5. Decreasing the time integration step to 0.005 second does not change the results. Increasing the viscous damping to 4% decreases the interstory drift, the maximum reduction being 17% between the 5th Floor and the Roof.

For Clad Frame B with 2% or 4% viscous damping, the total work dissipated by the frame at the end of the analysis (i.e., after 15 seconds of shaking) is approximately 5100 kip-in. With 2% damping, the dissipated viscous work is 31.1% of the total; the strain energy and dissipated hysteretic work is 65.1%; the kinetic energy is 3.5%; and the energy error is 0.3%. With 4% damping, the viscous work is 49.7% of the total; the strain energy and hysteretic work is 47.8%; the kinetic energy is 2.3%; and the energy error is 0.2%.

For linear analyses, viscous damping is used to approximate energy losses due to all causes. For nonlinear analyses, some or all of the elements behave hysteretically, and, hence, energy dissipation is modelled directly. However, a nonlinear model typically will not account for all sources of energy dissipation, and additional viscous damping will usually be specified. The amount of viscous damping should, however, be less than for a linear analysis. The amount of viscous damping for linear analyses can be determined by correlation with experiments for small amplitude shaking, and is typically increased to account for larger losses with stronger shaking. The appropriate amount of viscous damping for nonlinear analyses does not appear to have been decided.

In the present studies,with β corresponding to 2% damping at 1 second period, the amount of dissipated energy was approximately 5100 kip-in. Of this, somewhat less than 65% was hysteretic (since there was some elastic strain energy at the end of the analysis) and 31% was viscous. With β corresponding to 4% damping at 1 second period, the amount of dissipated energy was also approximately 5100 kip-in. Of this, somewhat less than 48% was hysteretic and 50% was viscous. A ratio of 2:1, hysteretic to viscous losses, as in the 2% case, may be reasonable, although intuition suggests the ratio should be larger (i.e., less viscous damping). A ratio of 1:1, as in the 4% case, certainly seems to overestimate the viscous losses. It is possible, therefore, that the analyses have over-estimated the amount of viscous damping. However, there do not appear to be any accepted guidelines. The question of the "correct" amount of viscous damping is a topic requiring further study. The assumption of 2% damping at 1 second period may be high, but is believed to be reasonable for the present study.

4.2.3 Maximum Plastic Hinge Rotations in Frames

For Clad Frame A designed using connection Concepts I, II, and III, the maximum plastic hinge rotations are given in Tables 4.8, 4.9, and 4.10. Some observations are as follows:

(1) All of the plastic hinge rotations are substantially smaller than for Frame R. The maximum value is 0.0088 radian for Concept I with $k_2/k_1 = 0.0$.

(1a) For Concept II, the maximum value is 0.0087 radian with $k_2/k_1 = 0.0$; for Concept III, the maximum value is 0.0033 radian with $k_2/k_1 = 0.0$.

(2) The plastic hinge rotations at the girder ends are not uniform throughout the height of the frame, with rotations at the Roof and 5th Floor significantly larger than for the lower floors. This correlates with the interstory drifts (see Table 4.3).

(3) There is slight hinging at the interior columns just above the 4th Floor, where the largest

girder hinge rotations occur.

(4) The introduction of 10% strain-hardening in the connections does not significantly decrease the magnitude of the plastic hinge rotations. These results are consistent with the observations about interstory drifts (see Section 4.2.2).

For Clad Frame B designed using connection Concepts I, II, and III, the maximum plastic hinge rotations are given in Tables 4.11, 4.12, and 4.13. Some observations are as follows:

(1) All of the plastic hinges are substantially smaller than for Frame R. The maximum value is 0.0071 radian for Concept II with $k_2/k_1 = 0.0$.

(1a) For Concept I, the maximum value is 0.0057 radian with $k_2/k_1 = 0.0$; for Concept III, the maximum value is 0.0035 radian with $k_2/k_1 = 0.0$.

(2) The plastic hinge rotations at the girder ends are not uniform throughout the height of the frame, with rotations at the Roof and 5th Floor significantly larger than for the lower floors. This correlates with the interstory drifts (see Table 4.4).

(3) The introduction of 10% strain-hardening in the connections does not significantly decrease the magnitude of the plastic hinge rotations. These results are consistent with the observations about interstory drifts (see Section 4.2.2).

For Clad Frame B designed using connection Concept III with 10% strain-hardening, the effects of two parameters on the plastic hinge rotations are shown in Table 4.14. Decreasing the time integration step to 0.005 second has little effect on the results. Increasing the viscous damping to 4% decreases the rotations and number of hinges.

4.2.4 Maximum Deformations and Maximum Ductility Ratios of Inelastic Top Panel Connections

The maximum deformation of the top inelastic panel connection is defined as δ_{max}. The maximum deformations of the inelastic top panel connections for Clad Frames A, B, and C, are given in Figs. 4.1a, 4.2a and 4.3a, and 4.4a, respectively.

The connection ductility ratio, μ, is defined as the maximum deformation, δ_{max}, divided by the yield ddeformation, δ_y. The maximum ductility ratios of the inelastic top panel connections for Clad Frames A, B, and C, are given in Figs. 4.1b, 4.2b and 4.3b, and 4.4b, respectively.

For Clad Frame A (see Figs. 4.1a and 4.1b), the following observations can be made:

(1) The maximum connection deformation is 1.90 inches for Concept I with $k_2/k_1 = 0.0$.

(1a) For Concept II, the maximum value is 1.87 inches with $k_2/k_1 = 0.0$; for Concept III, the maximum value is 1.32 inches with $k_2/k_1 = 0.1$.

(2) The maximum interstory drifts (from Table 4.3) are essentially equal to the maximum connection deformations.

(3) The maximum ductility ratio is 3.52 for Concept I with with $k_2/k_1 = 0.0$.

(3a) For Concept III, the maximum ratio is 2.44 with $k_2/k_1 = 0.0$ and $k_2/k_1 = 0.1$; for Concept II, the maximum ratio is 1.91 with $k_2/k_1 = 0.1$.

(4) The ductility ratios for Concept III are greater than those for Concept II and less than those for Concept I.

(5) The ductility ratios at the Roof are about twice as large as those at the 2nd Floor.

(5a) The ductility ratios are the most uniform for Concept III, where the ductility ratios at the Roof are about 1.8 times as large as those at the 2nd Floor.

(6) For Concept II, the ductility ratios at the 2nd Floor are less than 1.00, indicating that the connections remained elastic.

(7) The introduction of 10% strain-hardening does not significantly decrease the connection deformations in either the positive or negative directions.

For Clad Frame B (see Figs. 4.2a and 4.2b), the following observations can be made:

(1) The maximum connection deformation is 1.70 inches for Concepts I and II with $k_2/k_1 = 0.0$.

(1a) For Concept III, the maximum deformation is 1.30 inches with $k_2/k_1 = 0.0$.

(2) The maximum interstory drifts (from Table 4.4) are essentially equal to the maximum connection deformations.

(3) The maximum ductility ratio is 3.15 for Concept I with with $k_2/k_1 = 0.0$.

(3a) For Concept III, the maximum value is 2.43 with $k_2/k_1 = 0.0$ and $k_2/k_1 = 0.0$; for Concept II, the maximum value is 2.15 with $k_2/k_1 = 0.0$.

(4) The ductility ratios for Concept III are greater than those for Concept II and less than those for Concept I.

(5) The ductility ratios at the Roof are about 1.4 to 1.7 times as large as those at the 2nd Floor.

(5a) The ductility ratios are the most uniform for Concept III, where the ductility ratios at the Roof are about 1.4 times as large as those at the lowest story.

(6) For Concept II, the ductility ratios at the 2nd Floor are approximately equal to 1.00, indicating that there is minimal inelastic demand on the connections.

(7) The introduction of 10% strain-hardening does not significantly decrease the connection deformations in either the positive or negative directions.

For Clad Frame B designed using connection Concept III with 10% strain-hardening, the effects of two parameters on the deformations and ductility ratios are given in Figs. 4.3a and 4.3b, respectively. Decreasing the time integration step to 0.005 second has little effect on the results. Increasing the viscous damping to 4% decreases the ductility ratios, primarily in the upper floors.

For Clad Frame C (see Figs. 4.4a and 4.4b), the following observations can be made:

(1) The maximum connection deformation is 2.31 inches for Concept I with $k_2/k_1 = 0.0$.

(1a) For Concept II, the maximum value is 2.11 inches with $k_2/k_1 = 0.0$; for Concept III, the maximum value is 1.26 inches with $k_2/k_1 = 0.1$.

(2) The maximum interstory drifts (from Table 4.6) are essentially equal to the maximum connection deformations.

(3) The maximum ductility ratio is 4.28 for Concept I with with $k_2/k_1 = 0.0$.

(3a) For Concept III, the maximum ductility ratio is 2.61 with $k_2/k_1 = 0.0$ and $k_2/k_1 = 0.1$; for Concept II, the maximum ratio is 2.29 with $k_2/k_1 = 0.1$.

(4) The ductility ratios for Concept II are greater than those for Concept III and less than those for Concept I.

(5) The ductility ratios vary throughout the height of the frames. For Concept I, the largest values are found at the Roof, and the second largest values are found at the 2nd Floor with $k_2/k_1 = 0.0$ and at the 4th Floor with $k_2/k_1 = 0.1$. For Concept II, the ductility ratios decrease with decreasing height. For Concept III with $k_2/k_1 = 0.0$, the largest valeus are at the 4th Floor and the second largest values are at the 2nd Floor. For Concept III with $k_2/k_1 = 0.1$, the largest values are at the 2nd Floor, and the second largest values are at the 4th Floor.

(5a) The ductility ratios are the most uniform for Concept III, where the largest ductility ratios are 1.5 to 1.6 times as large as the smallest values.

(6) The smallest ductility ratio is 1.10 for Concept II with $k_2/k_1 = 0.0$, indicating that there is at least a minimal ductility demand on all connections.

(7) The introduction of 10% strain-hardening decreases some of the interstory drift ratios in the negative direction.

4.2.5 Maximum Forces in Elastic Side Panel Connections

The maximum forces in the elastic side panel connections for Clad Frames A, B, and C, are given in Figs. 4.5, 4.6 and 4.7,and 4.8, respectively. The forces in the connections at the exterior columns are typically several times larger than those at the interior columns. The forces tend to decrease with height. The largest connection force of 104 kips occurs between the 1st and 2nd Floors in Clad Frame C designed with Concept III and $k_2/k_1 = 0.1$ (see Fig. 4.8).

For Clad Frame B designed using connection Concept III with 10% strain-hardening, decreasing the time integration step to 0.005 second has a very minor effect on the results. Increasing the viscous damping to 4% slightly increases the magnitude of the forces in the connections.

4.2.6 Maximum Shear Forces in Panels

The maximum shear forces in the panels for Clad Frames A, B, and C, are recorded in this preliminary study for reference only and are given in Figs. 4.9, 4.10 and 4.11, and 4.12, respectively.

For Clad Frame B designed using connection Concept III with 10% strain-hardening, the effects of two parameters are given in Fig. 4.11. Decreasing the time integration step to 0.005 second has a very minor effect on the results. Increasing the viscous damping to 4% slightly increases the magnitude of the panel shear forces.

4.3 Effect of Strain-Hardening in Connections

In Sections 4.2.2, 4.2.3, and 4.2.4, it is noted that the introduction of 10% strain-hardening (i.e., $k_2/k_1 = 0.1$) for Clad Frames A and B with connection Concepts I, II, and III does not decrease the maximum interstory drifts, maximum plastic hinge rotations in the frames, or the maximum deformations in the cladding-to-frame connections. With strain-hardening, most of these quantities are slightly larger than without strain-hardening. This result is unexpected, since increased drifts are often observed for structures with zero-strain hardening.

The reason for this result is not clear, and is a subject for future study. One possible explanation is that the clad frames with strain-hardening connections are stiffer than those with no strain-hardening, resulting in smaller effective periods of vibration. With strain-hardening, the effective periods of the frames will be closer to the predominant period range of 0.25 to 1.00 second for the El Centro ground motion. The closer the structure's period is to the top of the response spectrum (i.e., higher up on the descending branch of the response spectrum), the larger the accelerations, and the larger the forces attracted to the structure. As a consequence, the drifts, etc., could tend to be larger for the stiffer clad frames with strain-hardening connections. A second possible explanation is that in Clad Frames A and B the frames remain partly elastic, and, hence, provide effective strain-hardening even with $k_2/k_1 = 0.0$. This explanation is supported to some extent by the fact that the results for $k_2/k_1 =$ 0.0 and 0.1 differ most for Clad Frame C, where the frame provides essentially no lateral stiffness.

4.4 Summary of Results

The results can be summarized as follows:

(1) The drifts for Clad Frames A, B, and C are generally smaller than for Frame R. The only exception is Clad Frame C with connection Concept I.

(2) The plastic hinge rotations in Clad Frames A and B are smaller than for Frame R.

(3) The drifts are reasonably uniform over the height of Clad Frames A, B, and C with Con-

cept III. There are some exceptions, including Frame R, and Clad Frames A, B and C with Concepts I and II.

(4) The plastic hinge rotations are not uniform over the height for either Frame R, or Clad Frames A, B, and C. The best example of well-distributed yielding is Clad Frame B with Concept II. The second best example is Clad Frame A with Concept II, but the columns just above the 4th Floor yield slightly.

(5) The ductility demands on the connections are more uniform over the height for Clad Frames A, B, and C with Concept III, than for Clad Frames A, B, and C with Concepts I and II. The worst example is Clad Frame C with Concept I and $k_2/k_1 = 0.0$.

(6) Typically, the behavior for Concepts I and II is very similar. Both of these concepts have the same initial stiffness, but Concept II has stronger connections. The maximum drifts, maximum interstory drift ratios, maximum plastic hinge rotations, and maximum deformations of the inelastic connections are about the same order of magnitude for both concepts. The only significant differences are for the maximum ductility ratios, which tend to be smaller for Concept II.

(7) Concept III has initially stiffer connections than Concepts I and II, but strengths equal to those of Concept II. Concept III generally has the smallest maximum drifts, maximum interstory drift ratios, maximum plastic hinge rotations, and maximum deformations of the inelastic connections. The maximum ductility ratios tend to be larger than those for Concept II and smaller than those for Concept I.

CHAPTER 5

CONCLUSION AND ASPECTS REQUIRING FURTHER STUDY

5.1 General Conclusions

This study has explored some basic aspects of the use of structural cladding panels with energy dissipating cladding-to-frame connections for seismic resistant design. A design procedure has been outlined, and three building frames have been designed using this procedure. Nonlinear dynamic analyses of the frames have indicated that they perform well. In particular, interstory drifts are smaller than for a comparably designed frame with nonstructural cladding. Plastic hinge rotations in the frame members are correspondingly reduced. The ductility demands on the cladding-to-frame connections are modest, and the forces transmitted to the cladding panels appear to be reasonable. Some aspects requiring further study are listed in the following section.

5.2 Aspects Requiring Further Study

The following aspects of analysis, design concept, retrofit, architectural design, and connection design require further study:

(1) Only one ground motion has been considered. More motions, including stronger motions, longer duration motions, and motions with other predominant frequencies need to be considered.

(2) Most analyses have been carried out assuming stiffness dependent (βK) damping, with β selected to give 2% damping at a period of 1 second. The analyses indicate that viscous energy dissipation in the model is about $^1/_3$ of the total, and hysteretic energy dissipation is about $^2/_3$ of the total (mainly in the cladding-to-frame connections). Intuitively, this $^1/_3$ figure for viscous dissipation seems to be rather high. The influence of β needs to be explored, and a reasonable level for viscous dissipation needs to be established.

(3) The design procedure used is this study needs to be refined and simplified. In particular, the following must be examined:

  (a) The yield deformation for the inelastic connections were chosen to be 0.00375h for Concepts I and III, 0.0068h for Frame A with Concept II, 0.0055h for Frame B with Concept II, and 0.0064h for Frame C with Concept II. These values were chosen rather arbitrarily, and may need to be modified.

  (b) The strengths in the connections were chosen to provide strengths comparable to that for a conventionally designed frame with nonstructural cladding. This is important, because a conventionally designed frame has an actual strength which substantially exceeds the nominal strength, whereas a frame with structural cladding has an actual strength closer to the nominal value (for Clad Frame C and zero strain-hardening in the connections, collapse occurs when the connections yield, with no "overstrength.") In order to obtain consistent strengths, it was necessary to perform nonlinear static push-over analyses, and to increase the nominal strengths for the clad frames. For practical design, appropriate amounts of overstrength could probably be identified, avoiding the need for the static push-over analysis.

(4) In this study, the connection strengths were changed from floor to floor, to match the design story shears. This might be impractical in an actual structure. The effect of changing the connection strength less frequently needs to be studied.

(5) The structure studied was only five stories tall. Taller structures need to be studied.

(6) The structure studied was of regular geometry with no set-backs. Structures with set-backs may pose special problems, for example, transfer of forces through the floor diaphragm from the cladding above the setback to the cladding below.

(7) Strengths, stiffnesses, and strain-hardening ratios have been chosen for the cladding-to-frame connections, but no attempt has been made to design practical connections with these properties. Design studies and tests are needed to determine whether practical devices can be designed.

(8) The panels in the study were not designed, and a weight of 35 psf was assumed. Procedures for panel design need to be established. The primary forces to be resisted by the panels are shear forces. However, the design is complicated by the fact that the forces from the connections may be exerted on the panels over only short lengths at the edges (e.g., the short "fin" connections at the vertical edges). The state of stress in a panel may thus be quite complex, especially for panels with window openings.

(9) The study has assumed that cladding will be present only in the perimeter framing. It may be possible that clad perimeter frames cannot provide adequate strength and stiffness. If plan aspect ratios are too large, then additional lateral resistance may be required in the shorter building direction. If so, it may be necessary to provide lateral resistance with interior panels. This will require different detailing for the panels and panel-to-frame connections.

(10) Retrofit of existing structures may pose problems for the attachment of the cladding-to-frame connections.

(11) At the ground floor, there may be architectural requirements for a different floor-to-floor height and for large door and window openings. This means that the use of structural panels may not

be possible. Other alternatives need to be sought for compatible strength, stiffness, ductility, and energy dissipation at the ground floor.

(12) The architectural design may include structural panels over only part of the facade. Facades with discontinuities in the structural cladding may pose special problems, for example, transfer of forces through the structural frame from the structural panels at each side of the discontinuity.

(13) Cladding panel design and detailing to accommodate windows need to be studied.

(14) Practical designs are needed for the elastic and inelastic cladding-to-frame connections. In addition to satisfying the structural requirements, these must meet physical dimension requirements, and must be easily installed, maintained, and inspected.

(15) The building envelope must be weather resistant. To accomplish this, it might be better to place the inelastic connections at the bottom of the panels, allowing for a simpler, more weatherproof connection at the top.

REFERENCES

AISC [1986], *Manual of Steel Construction: Load and Resistance Factor Design for Structural Steel Buildings (LRFD),* First Edition, Third Printing - 3/90, American Institute of Steel Construction, Inc., One East Wacker Drive, Suite 3100, Chicago, IL.

AISC [1990], "Seismic Provisions for Structural Steel Buildings - Load and Resistance Factor Design," Amer. Inst. of Steel Constr., Inc., One East Wacker Drive, Suite 3100, Chicago, IL., 15 Nov.

Allahabadi, R.; and Powell, G.H. [1988], "DRAIN-2DX User Guide," *Report No. UCB/EERC-88-06,* College of Engineering, Univ. of CA, Berkeley, March.

Clough, R.W.; and Penzien, J. [1975], *Dynamics of Structures,* McGraw-Hill Book Co., NY, 634 pp.

Davies, J.M.; and Bryan, E.R. [1982], *Manual of Stressed Skin Diaphragm Design,* John Wiley and Sons, Inc., NY.

Goodno, B.J.; and Palsson, H. [1986], "Analytical Studies of Building Cladding, *J. Struct. Div.*, ASCE, Vol. 112, No. 4, Apr. pp. 665-676.

Henry, R.M.; and Roll, F. [1986], "Cladding-Frame Interaction," *J. Struct. Div.,* ASCE, Vol. 112, No. 4, Apr., pp. 815-834.

Miller, C.J. [1972], "Analysis of Multistory Frames with Light Gauge Steel Panel Walls," *Report 349,* Dept. of Struct. Engrg., Cornell Univ., Ithaca, NY, Aug.

Pinelli, J.P.; Craig, J.I.; and Goodno, B.J. [1990a], "Development and Experimental Calibration of Selected Dynamic Models for Precast Cladding Connections," *Proc. Fourth U.S. Nat't Conf. on Earthquake Engrg.,* Vol. 2, Palm Springs, CA, pp.147-156, 20-24 May.

Pinelli, J.P.; Craig, J.I.; and Goodno, B.J. [1990b], *ATC-29: Seismic Design and Performance of Equipment and Nonstructural Elements in Bldgs and Industrial Structures,* Irvine, CA, pp. 26-1 - 26-11, 3-4 Oct.

Powell, G.H. [1990], "DRAIN-2DX Version 0.01 USER GUIDE," Dept. of Civil Engrg., Univ. of CA, Berkeley, CA, Nov.

Precast/Prestressed Concrete Institute (PCI) [1989], "Architectural Precast Concrete Cladding - Its Contribution to Lateral Resistance of Buildings," *Proc.,* Chicago, IL, 8-9 Nov.

SEAOC [1990], "Recommended Lateral Force Requirements and Commentary," Seismology Committee, Structural Engineers Association of California, P.O. Box 19440, Sacramento, CA.

Tomasetti, R.L.; Gutman, A.; Lew I.P.; and Joseph, L.M. [1986a], "Development of Thin Wall Cladding to Reduce Drift in Hi-Rise Buildings," *IABSE Colloquium Proceedings,* Vol. 49, pp. 239-246.

Tomasetti, R.L.; Gutman, A.; Lew I.P.; and Joseph, L.M. [1986b], "A Stressed-Skin Tube Tower: One Mellon Bank Center," *Advances in Tall Buildings,* Council on Tall Buildings and Urban Habitat, Edited by L.S. Beedle, Van Nostrand Reinhold Co., NY, pp. 573-605.

Tomasetti, R.L.; Gutman, A.; Joseph, L.M.; and Beer, D. [1984], "One Mellon Bank Center: The Skin is More than Beauty Deep," *Modern Steel Construction,* 3rd Quarter, pp. 5-10.

UBC [1991], *Uniform Building Code,* First Printing, International Conference of Building Officials, 5360 South Workman Mill Road, Whittier, CA, 1 May.

Unclad Frame	Floor	Lateral Loads (kips)	Story Shears (kips)
Frame R	Roof	52.9 + 10.6 = 63.5	63.5
	5th	54.6	118.
	4th	41.0	159.
	3rd	27.3	186.
	2nd	13.7	200.
Frame A	Roof	35.2 + 7.07 = 42.3	42.3
	5th	36.4	78.7
	4th	27.3	106.
	3rd	18.2	124.
	2nd	9.33	133.
Frame B	Roof	13.2 + 2.65 = 15.9	15.9
	5th	13.7	29.5
	4th	10.3	39.8
	3rd	6.83	46.5
	2nd	3.43	50.0

Table 2.1 Nominal Design Loads, 1.0E, for Unclad Frames

Unclad Frame	Design Load Level	Design Load	Design Load, $n \times (1.5E_R)$	Required Connection Strength $(n-1) \times 1.5E_R$
Frame R	$R_w = 8$ 100% Lateral Strength	$1.0\ (1.5E_R)$	$1.0\ (1.5E_R)$	$0.0\ (1.5E_R)$
Frame A	$R_w = 12$ 100% Lateral Strength (equivalent to $R_w = 8$ for $66^2/3$% Lateral Strength)	$0.67\ (1.5E_A)$	$0.67\ (1.5E_R)$	$0.33\ (1.5E_R)$
Frame B	$R_w = 8$ 25% Lateral Strength	$0.25\ (1.5E_B)$	$0.25\ (1.5E_R)$	$0.75\ (1.5E_R)$
Frame C	0% Lateral Strength	0.0	$0.0\ (1.5E_R)$	$1.0\ (1.5E_R)$

Table 2.2a Concept I: Required Top Panel Connection Strength for Clad Frames Designed for 0% Overstrength of Frame R

Floor	$1.5E_R$ (kips)	Frame A $0.33(1.5E_R)$ (kips)	Frame B $0.75(1.5E_R)$ (kips)	Frame C $1.0(1.5E_R)$ (kips)
Roof	95.3	31.7	71.4	95.3
5th Floor	177.	59.0	133.	177.
4th Floor	239.	79.5	179.	239.
3rd Floor	279.	93.0.	209.	279.
2nd Floor	300.	100.	225.	300.

Table 2.2b Concept I: Additional Story Strengths Needed in Inelastic Top Panel Connections for Clad Frames Designed for 0% Overstrength of Frame R

Floor	Frame A K_1 for $0.33(1.5E_R)$ (kip/in)	Frame B K_1 for $0.75(1.5E_R)$ (kip/in)	Frame C K_1 for $1.0(1.5E_R)$ (kip/in)
Roof	58.7	132.	176.
5th Floor	109.	246.	328.
4th Floor	147.	331.	443.
3rd Floor	172.	387.	517.
2nd Floor	185.	417.	555.

Table 2.2c Concept I: Elastic Stiffnesses for Inelastic Top Panel Connections with δ_y = 0.00375 h for Clad Frames Designed for 0% Overstrength of Frame R

Unclad Frame	Design Level	Collapse Load / Design Load 1.5E	Collapse Load / Design Load ($1.5E_R$)	Required Connection Strength, x ($1.5E_R$) (kips)
Frame R	$R_w = 8$ 100% Lateral Strength	2.537/1.5 = 1.692	1.70	0.000 ($1.5E_R$)
Frame A	$R_w = 12$ 100% Lateral Strength (equivalent to $R_w = 8$ for $66^2/3$% Lateral Strength)	2.488/1.5 = 1.659	1.10	0.60 ($1.5E_R$)
Frame B	$R_w = 8$ 25% Lateral Strength	3.575/1.5 = 2.383	0.60	1.10 ($1.5E_R$)
Frame C	0% Lateral Strength	0.000	0.000	1.419 ($1.5E_R$)

Table 2.3a Concept II: Required Top Panel Connection Strength for Clad Frames Designed for 70% Overstrength from Frame R

Floor	$(1.5E_R)$ (kips)	Frame A $0.60(1.5E_R)$ (kips)	Frame B $1.10(1.5E_R)$ (kips)	Frame C $1.70(1.5E_R)$ (kips)
Roof	95.3	57.2	105.	162.
5th Floor	177.	106.	195.	301.
4th Floor	239.	143.	263.	406.
3rd Floor	279.	167.	307.	474.
2nd Floor	300.	180.	330.	510.

Table 2.3b Concept II: Additional Story Strengths Needed in Inelastic Top Panel Connections for Clad Frames Designed for 70% Overstrength from Frame R

Floor	Frame A K_1 (kip/in.) and δ_y/h for $0.60(1.5E_R)$		Frame B K_1 (kips/in.) and δ_y/h for $1.10(1.5E_R)$		Frame C K_1 (kip/in.) and δ_y/h for $1.70(1.5E_R)$	
Roof	58.7	0.0068	132.	0.0055	176.	0.0064
5th Floor	109.	0.0068	246.	0.0055	328.	0.0064
4th Floor	147.	0.0068	331.	0.0055	443.	0.0064
3rd Floor	172.	0.0068	387.	0.0055	517.	0.0064
2nd Floor	185.	0.0068	417.	0.0055	555.	0.0064

Table 2.3c Concept II: Yield Displacements for Inelastic Top Panel Connections for Clad Frames Designed for 70% Overstrength from Frame R

Floor	$(1.5E_R)$ (kips)	Frame A $0.60(1.5E_R)$ (kips)	Frame B $1.10(1.5E_R)$ (kips)	Frame C $1.70(1.5E_R)$ (kips)
Roof	95.3	57.2	105.	162.
5th Floor	177.	106.	195.	301.
4th Floor	239.	143.	263.	406.
3rd Floor	279.	167.	307.	474.
2nd Floor	300.	180.	330.	510.

Table 2.4a Concept III: Additional Story Strengths Needed in Inelastic Top Panel Connections for Clad Frames Designed for 70% Overstrength from Frame R

Floor	Frame A δ_y/h and K_1 (kips/in.) for $0.60(1.5E_R)$		Frame B δ_y/h and K_1 (kips/in.) for $1.10(1.5E_R)$		Frame C δ_y/h and K_1 (kips/in.) for $1.70(1.5E_R)$	
Roof	0.00375	106.	0.00375	194.	0.00375	300.
5th Floor	0.00375	197.	0.00375	361.	0.00375	557.
4th Floor	0.00375	266.	0.00375	487.	0.00375	752.
3rd Floor	0.00375	310.	0.00375	568.	0.00375	878.
2nd Floor	0.00375	333.	0.00375	611.	0.00375	944.

Table 2.4b Concept III: Elastic Stiffnesses for Inelastic Top Panel Connections with δ_y = 0.00375 h for Clad Frames Designed for 70% Overstrength from Frame R

Frame	Concept for P_y, K_1 and δ_y for Top Panel Connections	Fundamental Period (sec.)
Frame R	n/a	0.991
Clad Frame A	I	1.293
	II	1.293
	III	1.132
Clad Frame B	I	1.211
	II	1.211
	III	1.052
Clad Frame C	I	1.242
	II	1.242
	III	0.987

Table 4.1 Elastic Fundamental Periods of Reference Frame R, and Clad Frames A, B, and C

Floors	$+\delta$ (in.)	$+\delta/h$	Time (sec.)	$-\delta$ (in.)	$-\delta/h$	Time (sec.)
5th - Roof	2.27	0.0157	8.93	-1.56	-0.0108	5.88
4th - 5th	1.74	0.0121	8.86	-1.33	-0.0092	5.88
3rd - 4th	1.11	0.0077	8.79	-0.92	-0.0064	5.85
2nd - 3rd	0.94	0.0066	8.70	-0.84	-0.0058	5.77
1st - 2nd	0.81	0.0056	8.64	-0.73	-0.0050	5.77

Table 4.2 Envelopes of Interstory Drifts (δ) and Interstory Drift Ratios (δ/h) for Frame R

Concept for P_y, K_1 and δ_y for Top Panel Conns.	Floors	Inelastic Top Panel Connections with k_2/k_1 = 0.0						Inelastic Top Panel Connections with k_2/k_1 = 0.1					
		+δ (in.)	+δ/h	Time (sec.)	-δ (in.)	-δ/h	Time (sec.)	+δ (in.)	+δ/h	Time (sec.)	-δ (in.)	-δ/h	Time (sec.)
I	5th - Roof	1.07	0.0074	2.46	-1.90	-0.0132	2.18	1.11	0.0079	2.46	-1.87	-0.0130	2.17
	4th - 5th	0.99	0.0069	6.12	-1.80	-0.0125	2.14	1.04	0.0074	6.11	-1.78	-0.0123	2.14
	3rd - 4th	1.04	0.0072	6.02	-1.18	-0.0082	2.08	1.06	0.0074	6.02	-1.17	-0.0081	2.08
	2nd - 3rd	1.11	0.0077	6.02	-1.00	-0.0070	3.03	1.12	0.0078	6.00	-0.99	-0.0069	3.02
	1st - 2nd	0.75	0.0052	6.04	-0.71	-0.0049	5.14	0.76	0.0053	6.03	-0.70	-0.0048	2.96
II	5th - Roof	1.13	0.0079	2.45	-1.88	-0.0130	5.38	1.18	0.0082	2.44	-1.84	-0.0128	2.15
	4th - 5th	1.29	0.0089	6.11	-1.71	-0.0119	5.41	1.36	0.0094	6.11	-1.68	-0.0117	2.12
	3rd - 4th	1.23	0.0085	6.11	-1.33	-0.0092	3.09	1.25	0.0087	6.11	-1.32	-0.0092	3.09
	2nd - 3rd	1.19	0.0083	6.03	-1.12	-0.0078	6.71	1.19	0.0083	6.03	-1.13	-0.0078	6.71
	1st - 2nd	0.85	0.0059	6.01	-0.83	-0.0057	6.69	0.85	0.0059	6.01	-0.84	-0.0058	6.69
III	5th - Roof	1.30	0.0091	2.44	-1.26	-0.0087	2.09	1.33	0.0092	2.44	-1.25	-0.0087	2.09
	4th - 5th	1.17	0.0081	6.00	-1.32	-0.0092	2.10	1.23	0.0085	5.99	-1.29	-0.0090	2.09
	3rd - 4th	1.11	0.0077	5.94	-1.16	-0.0080	3.05	1.13	0.0079	5.94	-1.18	-0.0082	3.05
	2nd - 3rd	1.06	0.0074	5.89	-1.06	-0.0073	3.00	1.09	0.0075	5.89	-1.07	-0.0074	3.01
	1st - 2nd	0.73	0.0051	5.85	-0.71	-0.0049	2.94	0.77	0.0053	5.84	-0.71	-0.0049	2.94

Table 4.3 Envelopes of Interstory Drifts (δ) and Interstory Drift Ratios (δ/h) for Clad Frame A

Concept for P_y, K_1 and δ_y for Top Panel Conns.	Floors	Inelastic Top Panel Connections with k_2/k_1 = 0.0						Inelastic Top Panel Connections with k_2/k_1 = 0.1					
		$+\delta$ (in.)	$+\delta/h$	Time (sec.)	$-\delta$ (in.)	$-\delta/h$	Time (sec.)	$+\delta$ (in.)	$+\delta/h$	Time (sec.)	$-\delta$ (in.)	$-\delta/h$	Time (sec.)
I	5th - Roof	1.02	0.0071	2.47	-1.26	-0.0087	2.11	1.10	0.0077	2.47	-1.27	-0.0088	2.11
	4th - 5th	0.86	0.0060	12.11	-1.71	-0.0119	2.15	0.92	0.0064	12.11	-1.65	-0.0114	2.14
	3rd - 4th	0.83	0.0058	6.03	-1.36	-0.0094	3.11	0.97	0.0068	6.02	-1.25	-0.0087	3.10
	2nd - 3rd	0.79	0.0055	5.95	-1.31	-0.0091	3.03	0.93	0.0065	5.95	-1.18	-0.0082	3.03
	1st - 2nd	0.51	0.0035	13.18	-0.88	-0.0061	2.97	0.60	0.0041	5.91	-0.85	-0.0059	2.96
II	5th - Roof	1.10	0.0077	2.45	-1.53	-0.0106	5.37	1.15	0.0080	2.44	-1.48	-0.0103	5.36
	4th - 5th	1.01	0.0070	12.09	-1.70	-0.0118	5.38	1.16	0.0081	12.08	-1.58	-0.0110	5.37
	3rd - 4th	1.17	0.0081	6.01	-1.61	-0.0119	3.10	1.29	0.0090	6.00	-1.54	-0.0107	3.09
	2nd - 3rd	1.25	0.0087	5.92	-1.36	-0.0094	3.03	1.32	0.0092	5.92	-1.30	-0.0091	3.03
	1st - 2nd	0.83	0.0058	5.85	-0.87	-0.0060	2.94	0.87	0.0061	5.85	-0.87	-0.0060	2.94
III	5th - Roof	1.05	0.0073	2.44	-0.88	-0.0063	2.05	1.08	0.0075	2.44	-0.91	-0.0063	2.05
	4th - 5th	1.31	0.0091	12.12	-1.09	-0.0075	2.09	1.16	0.0081	5.90	-1.18	-0.0073	2.08
	3rd - 4th	1.24	0.0086	5.86	-1.26	-0.0088	3.04	1.15	0.0080	5.84	-1.23	-0.0086	3.03
	2nd - 3rd	1.21	0.0084	4.47	-1.22	-0.0084	3.01	1.19	0.0083	4.47	-1.18	-0.0082	3.01
	1st - 2nd	0.73	0.0051	4.41	-0.78	-0.0054	2.94	0.76	0.0053	4.41	-0.80	-0.0056	2.94

Table 4.4 Envelopes of Interstory Drifts (δ) and Interstory Drift Ratios (δ/h) for Clad Frame B

Parameters	Floors	+δ (in.).	+δ/h	Time (sec.)	-δ (in.)	-δ/h	Time (sec.)
Δt = 0.01 sec.	5th - Roof	1.08	0.0075	2.44	-0.91	-0.0063	2.05
ξ = 2%	4th - 5th	1.16	0.0081	5.90	-1.18	-0.0073	2.08
	3rd - 4th	1.15	0.0080	5.84	-1.23	-0.0086	3.03
	2nd - 3rd	1.19	0.0083	4.47	-1.18	-0.0082	3.01
	1st - 2nd	0.76	0.0053	4.41	-0.80	-0.0056	2.94
Δt = 0.005 sec.	5th - Roof	1.08	0.0075	2.44	-0.91	-0.0063	2.05
ξ = 2%	4th - 5th	1.17	0.0081	5.90	-1.06	-0.0073	2.08
	3rd - 4th	1.16	0.0080	5.85	-1.23	-0.0085	3.04
	2nd - 3rd	1.20	0.0083	4.47	-1.18	-0.0082	3.01
	1st - 2nd	0.77	0.0053	4.42	-0.80	-0.0056	2.94
Δt = 0.01 sec.	5th - Roof	0.93	0.0064	2.42	-0.79	-0.0055	2.05
ξ = 4%	4th - 5th	1.03	0.0072	12.09	-0.93	-0.0066	3.01
	3rd - 4th	1.10	0.0076	4.50	-1.16	-0.0081	3.02
	2nd - 3rd	1.17	0.0081	4.46	-1.17	-0.0081	2.99
	1st - 2nd	0.78	0.0054	4.42	-0.78	-0.0054	2.95

Table 4.5 **Envelopes of Interstory Drifts (δ) and Interstory Drift Ratios (δ/h) for Clad Frame B with Design Concept III and k_2/k_1 = 0.1 for Inelastic Top Panel Connections**

Concept for P_y, K_1 and δ_y for Top Panel Conns.	Floors	Inelastic Top Panel Connections with k_2/k_1 = 0.0						Inelastic Top Panel Connections with k_2/k_1 = 0.1					
		+δ (in.)	+δ/h	Time (sec.)	-δ (in.)	-δ/h	Time (sec.)	+δ (in)	+δ/h	Time (sec.)	-δ (in.)	-δ/h	Time (sec.)
I	5th - Roof	1.03	0.0071	4.70	-2.27	-0.0158	2.26	1.33	0.0093	2.59	-2.10	-0.0146	2.23
	4th - 5th	1.15	0.0078	14.59	-2.05	-0.0143	3.11	1.28	0.0089	12.16	-1.59	-0.0114	2.18
	3rd - 4th	0.92	0.0064	14.54	-1.40	-0.0097	3.09	1.00	0.0069	5.98	-1.06	-0.0074	3.00
	2nd - 3rd	1.02	0.0071	14.54	-0.85	-0.0059	3.04	0.77	0.0053	14.56	-1.08	-0.0075	3.09
	1st - 2nd	0.52	0.0036	1.57	-2.10	-0.0146	5.42	0.75	0.0052	14.54	-1.47	-0.0102	5.37
II	5th - Roof	1.63	0.0113	4.67	-2.09	-0.0145	2.19	1.67	0.0116	2.52	-1.99	-0.0139	2.18
	4th - 5th	0.69	0.0048	3.63	-2.10	-0.0146	5.47	1.12	0.0078	14.59	-1.71	-0.0119	5.44
	3rd - 4th	1.33	0.0092	6.03	-1.11	-0.0077	5.39	1.28	0.0089	5.99	-1.12	-0.0078	5.39
	2nd - 3rd	1.19	0.0082	6.03	-1.11	-0.0077	3.04	1.25	0.0087	6.02	-1.09	-0.0076	3.04
	1st - 2nd	1.16	0.0080	14.52	-1.23	-0.0085	3.08	1.22	0.0085	6.05	-1.22	-0.0085	3.07
III	5th - Roof	1.02	0.0071	2.44	-0.93	-0.0065	2.06	1.08	0.0075	2.44	-0.94	-0.0065	4.87
	4th - 5th	1.42	0.0099	12.08	-0.83	-0.0058	2.05	1.27	0.0088	2.42	-0.82	-0.0057	2.04
	3rd - 4th	0.93	0.0064	2.35	-0.87	-0.0060	2.94	0.92	0.0064	2.35	-0.92	-0.0064	2.94
	2nd - 3rd	0.77	0.0054	11.99	-1.10	-0.0076	2.97	1.13	0.0079	4.48	-1.04	-0.0072	2.94
	1st - 2nd	1.25	0.0087	4.46	-1.26	-0.0088	2.99	1.43	0.0099	4.44	-1.23	-0.0085	2.97

Table 4.6 Envelopes of Interstory Drifts (δ) and Interstory Drift Ratios (δ/h) for Clad Frame C

	Col.	Girder End	Girder End	Col.	Girder End	Girder End	Col.	Girder End	Girder End	Col.
Roof		0.0124	0.0056		0.0114	0.0015		0.0121	0.0065	
5th		0.0095	0.0043			0.0042		0.0082	0.0053	
4th		0.0030			0.0011			0.0014	0.0001	
3rd										
2nd		0.0003								
1st							0.0000			

Table 4.7 Frame R: Envelopes of Plastic Hinge Rotations (rad.)

with k_2/k_1 = 0.0 for inelastic top panel connections:

	Col.	Girder End	Girder End	Col.	Girder End	Girder End	Col.	Girder End	Girder End	Col.
Roof		0.0034	0.0074		0.0024	0.0067		0.0029	0.0080	
5th		0.0024	0.0078		0.0012	0.0077		0.0010	0.0088	
				0.0005			0.0005			
4th		0.0003	0.0022			0.0018			0.0036	
3rd		0.0009							0.0001	
2nd		0.0004								
1st										

with k_2/k_1 = 0.1 for inelastic top panel connections:

	Col.	Girder End	Girder End	Col.	Girder End	Girder End	Col.	Girder End	Girder End	Col.
Roof		0.0039	0.0069		0.0029	0.0064		0.0034	0.0075	
5th		0.0032	0.0076		0.0020	0.0076		0.0017	0.0086	
				0.0004			0.0004			
4th		0.0006	0.0021			0.0016		0.0002	0.0034	
3rd		0.0010						0.0002	0.0000	
2nd		0.0004								
1st										

Table 4.8 Clad Frame A, Concept I: Envelopes of Plastic Hinge Rotations (rad.)

with k_2/k_1 = 0.0 for inelastic top panel connections:

	Col.	Girder End	Girder End	Col.	Girder End	Girder End	Col.	Girder End	Girder End	Col.
Roof		0.0036	0.0079		0.0026	0.0074		0.0031	0.0087	
5th		0.0042	0.0075		0.0032	0.0075		0.0027	0.0085	
				0.0001			0.0001			
4th		0.0027	0.0023		0.0009	0.0019		0.0012	0.0036	
3rd		0.0020	0.0009		0.0006	0.0006		0.0013	0.0018	
2nd		0.0014	0.0008					0.0007	0.0013	
1st										

with k_2/k_1 = 0.1 for inelastic top panel connections:

	Col.	Girder End	Girder End	Col.	Girder End	Girder End	Col.	Girder End	Girder End	Col.
Roof		0.0039	0.0073		0.0030	0.0068		0.0035	0.0080	
5th		0.0048	0.0070		0.0038	0.0000		0.0034	0.0079	
				0.0000			0.0000			
4th		0.0030	0.0022		0.0012	0.0019		0.0015	0.0035	
3rd		0.0021	0.0008		0.0007	0.0005		0.0014	0.0017	
2nd		0.0014	0.0009		0.0000			0.0008	0.0014	
1st										

Table 4.9 Clad Frame A, Concept II: Envelopes of Plastic Hinge Rotations (rad.)

with k_2/k_1 = 0.0 for inelastic top panel connections:

	Col.	Girder End	Girder End	Col.	Girder End	Girder End	Col.	Girder End	Girder End	Col.
Roof		0.0023	0.0006		0.0019	0.0004		0.0022	0.0007	
5th		0.0029	0.0023		0.0019	0.0024		0.0022	0.0031	
4th		0.0004	0.0001					0.0000	0.0010	
3rd			0.0000					0.0002	0.0008	
2nd										
1st										

with k_2/k_1 = 0.1 for inelastic top panel connections:

	Col.	Girder End	Girder End	Col.	Girder End	Girder End	Col.	Girder End	Girder End	Col.
Roof		0.0025	0.0005		0.0020	0.0004		0.0024	0.0004	
5th		0.0033	0.0021		0.0023	0.0022		0.0026	0.0028	
4th		0.0008	0.0004			0.0001		0.0003	0.0013	
3rd		0.0009	0.0002					0.0004	0.0010	
2nd										
1st										

Table 4.10 Clad Frame A, Concept III: Envelopes of Plastic Hinge Rotations (rad.)

with $k_2/k_1 = 0.0$ for inelastic top panel connections:

	Col.	Girder End	Girder End	Col.	Girder End	Girder End	Col.	Girder End	Girder End	Col.
Roof										
5th		0.0003	0.0048			0.0048			0.0055	
4th		0.0006	0.0049			0.0048		0.0002	0.0057	
3rd			0.0029			0.0028			0.0035	
2nd			0.0026			0.0023			0.0029	
1st										

with $k_2/k_1 = 0.1$ for inelastic top panel connections:

	Col.	Girder End	Girder End	Col.	Girder End	Girder End	Col.	Girder End	Girder End	Col.
Roof								0.0000		
5th		0.0014	0.0045		0.0006	0.0045		0.0009	0.0052	
4th		0.0014	0.0044		0.0006	0.0044		0.0010	0.0051	
3rd		0.0008	0.0017		0.0003	0.0015		0.0006	0.0021	
2nd			0.0018			0.0014			0.0020	
1st										

Table 4.11 Clad Frame B, Concept I: Envelopes of Plastic Hinge Rotations (rad.)

with k_2/k_1 = 0.0 for inelastic top panel connections:

	Col.	Girder End	Girder End	Col.	Girder End	Girder End	Col.	Girder End	Girder End	Col.
Roof			0.0022			0.0020			0.0023	
5th		0.0017	0.0064		0.0010	0.0064		0.0011	0.0071	
4th		0.0034	0.0001		0.0026	0.0052		0.0029	0.0058	
3rd		0.0043	0.0045		0.0035	0.0045		0.0037	0.0001	
2nd		0.0033	0.0020		0.0025	0.0018		0.0031	0.0023	
1st										

with k_2/k_1 = 0.1 for inelastic top panel connections:

	Col.	Girder End	Girder End	Col.	Girder End	Girder End	Col.	Girder End	Girder End	Col.
Roof		0.0000	0.0020			0.0018		0.0001	0.0021	
5th		0.0023	0.0057		0.0016	0.0056		0.0017	0.0064	
4th		0.0045	0.0048		0.0037	0.0048		0.0039	0.0055	
3rd		0.0049	0.0038		0.0041	0.0039		0.0043	0.0045	
2nd		0.0039	0.0019		0.0030	0.0016		0.0036	0.0021	
1st										

Table 4.12 Clad Frame B, Concept II: Envelopes of Plastic Hinge Rotations (rad.)

with k_2/k_1 = 0.0 for inelastic top panel connections:

	Col.	Girder End	Girder End	Col.	Girder End	Girder End	Col.	Girder End	Girder End	Col.
Roof		0.0014								
5th		0.0019						0.0016		
4th		0.0034	0.0010		0.0029	0.0009		0.0030	0.0013	
3rd		0.0035	0.0026		0.0027	0.0026		0.0029	0.0031	
2nd		0.0018	0.0014		0.0011	0.0011		0.0017	0.0016	
1st										

with k_2/k_1 = 0.1 for inelastic top panel connections:

	Col.	Girder End	Girder End	Col.	Girder End	Girder End	Col.	Girder End	Girder End	Col.
Roof										
5th		0.0015			0.0012			0.0010		
4th		0.0025	0.0013		0.0020	0.0013		0.0021	0.0017	
3rd		0.0032	0.0021		0.0025	0.0021		0.0027	0.0026	
2nd		0.0019	0.0013		0.0012	0.0010		0.0017	0.0015	
1st										

Table 4.13 Clad Frame B, Concept III: Envelopes of Plastic Hinge Rotations (rad.)

with Δt = 0.005 sec. and ξ = 2%:

	Col.	Girder End	Girder End	Col.	Girder End	Girder End	Col.	Girder End	Girder End	Col.
Roof										
5th		0.0015			0.0012			0.0010		
4th		0.0025	0.0013		0.0021	0.0013		0.0021	0.0017	
3rd		0.0032	0.0021		0.0025	0.0021		0.0027	0.0026	
2nd		0.0019	0.0013		0.0012	0.0009		0.0018	0.0015	
1st										

with Δt = 0.01 sec. and ξ = 4%:

	Col.	Girder End	Girder End	Col.	Girder End	Girder End	Col.	Girder End	Girder End	Col.
Roof										
5th		0.0000								
4th		0.0005	0.0006		0.0002	0.0006		0.0003	0.0009	
3rd		0.0023	0.0016		0.0018	0.0016		0.0020	0.0021	
2nd		0.0018	0.0012		0.0011	0.0009		0.0017	0.0014	
1st										

Table 4.14 Clad Frame B, Concept III, k_2/k_1 = 0.1: Envelopes of Plastic Hinge Rotations (rad.)

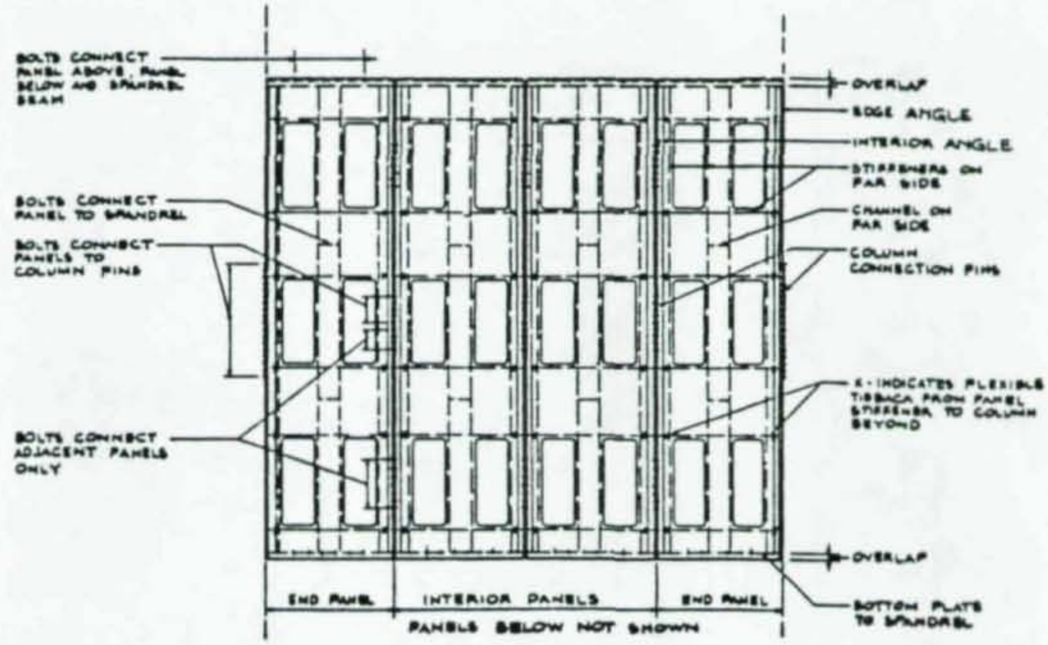

Fig. 1.1a Typical Elev. of Cladding Panel from One Mellon Center
with column covers removed. Diagonal face shown.
(from Tomasetti, et al. [1984], [1986a,b])

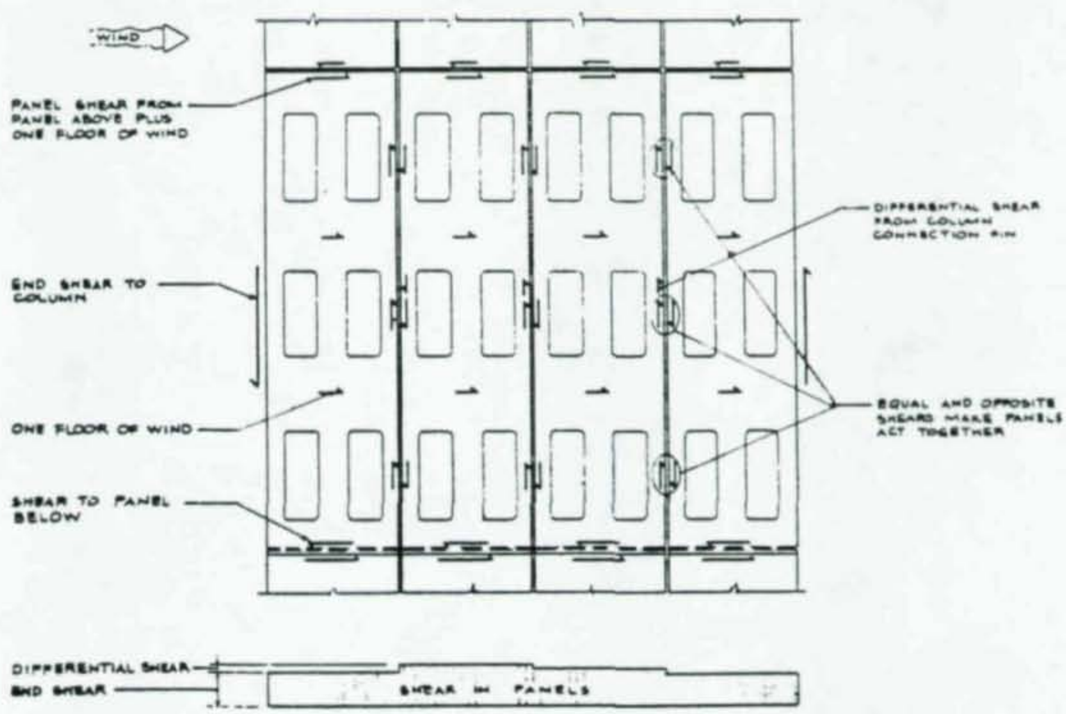

Fig. 1.1b Forces Acting on Cladding Panel from One Mellon Center
(from Tomasetti, et al. [1984], [1986a,b])

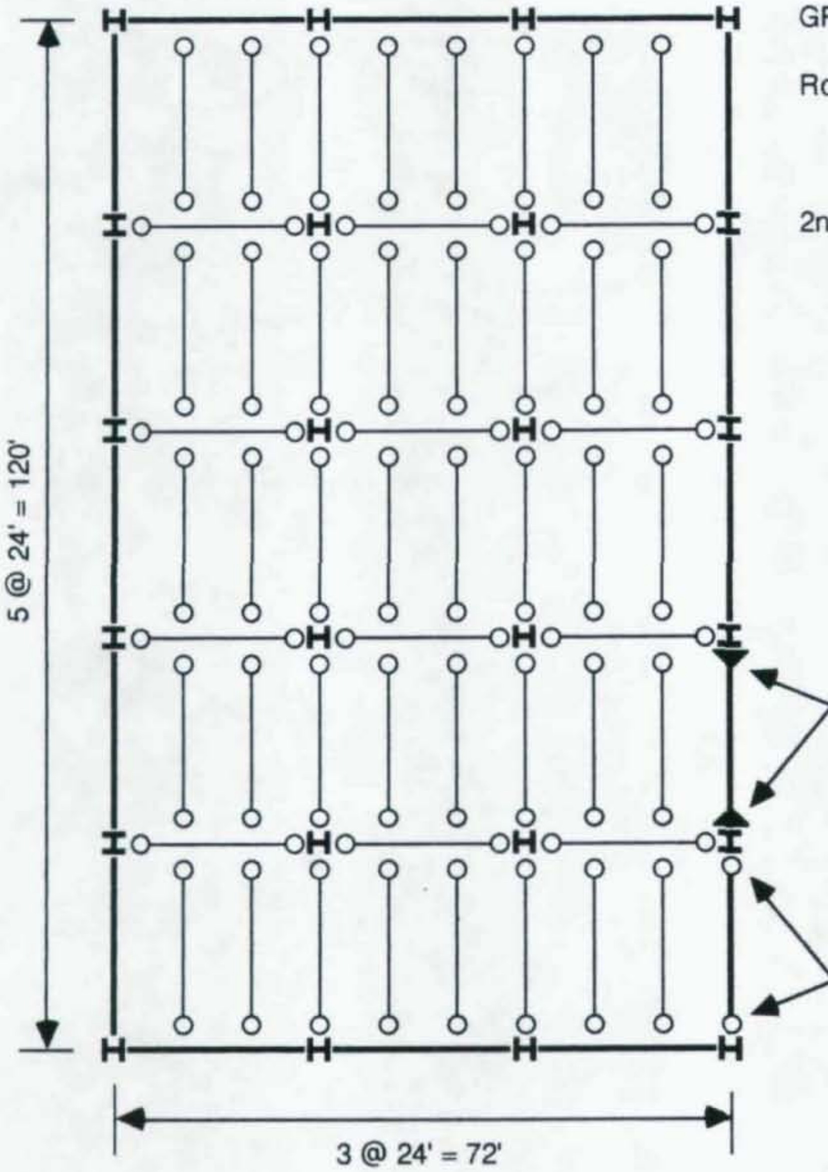

GRAVITY LOADS -

Roof:
Dead Load = D = 90 psf
Live Load = L = 0 psf

2nd - 5th Floors:
Dead Load = D = 110 psf
Live Load = L = 50 psf nominal;
L = 45 psf reduced for perimeter transverse girders

Moment-Resisting Girder-Column Connections for Perimeter Girders of Reference Frame R, and Frames A and B

Simple Girder-Column Connections for Perimeter Girders of Frame C

Fig. 2.1 Floor Framing and Gravity Loads

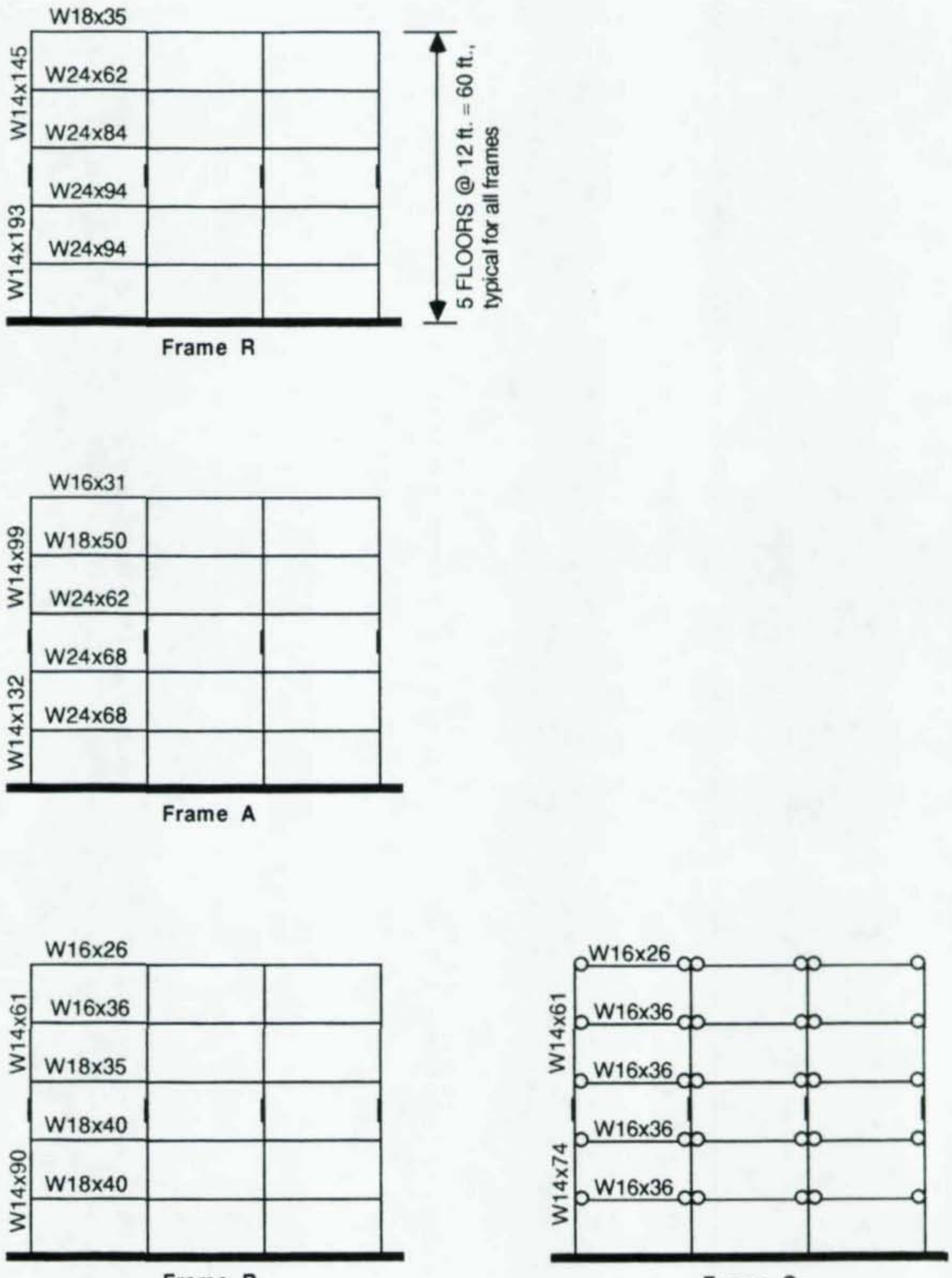

Fig. 2.2 Member Sizes for Reference Frame R, and Unclad Frames A, B, and C

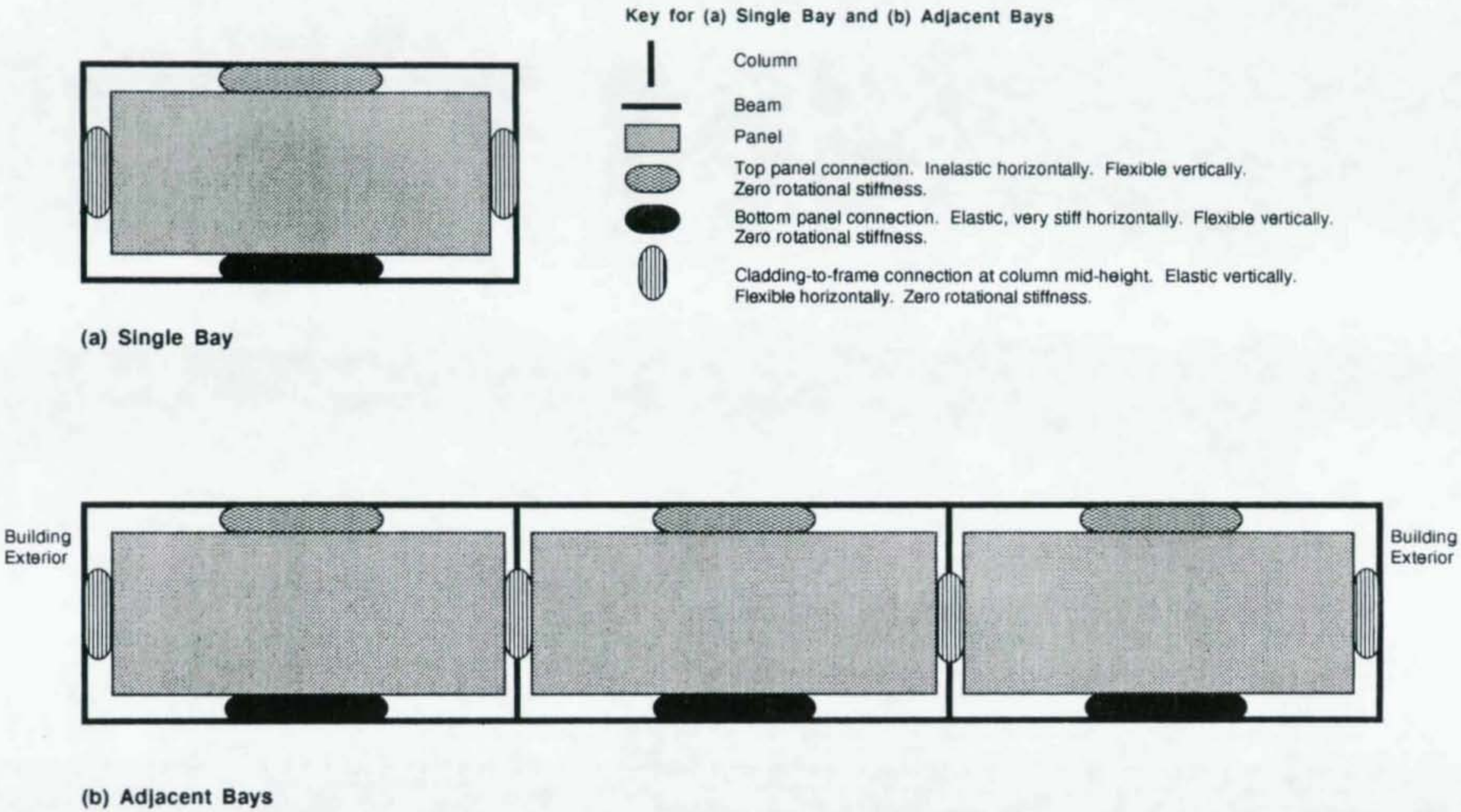

Fig. 2.3 Design Concept for Cladding Connections

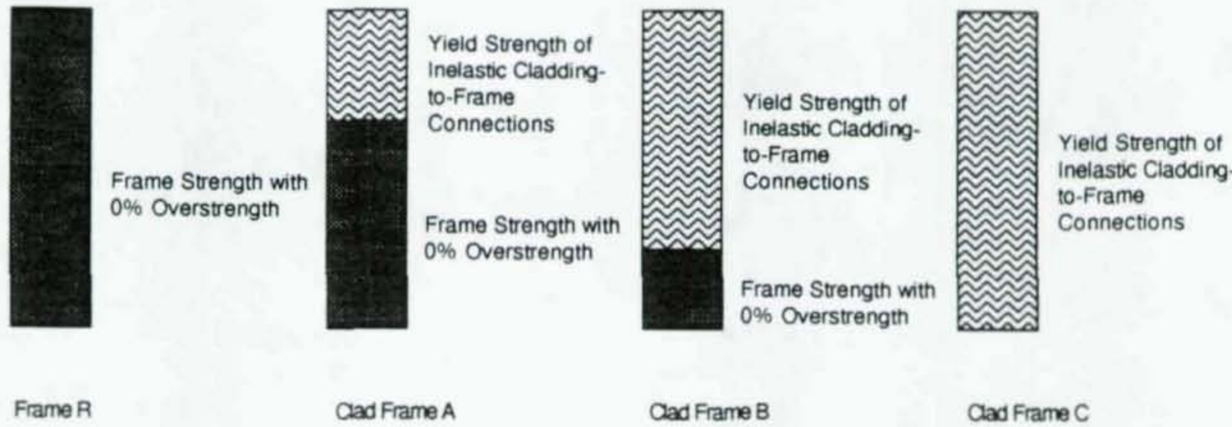

Fig. 2.4a Frame and Connection Strengths based on Frame R with 0% Overstrength

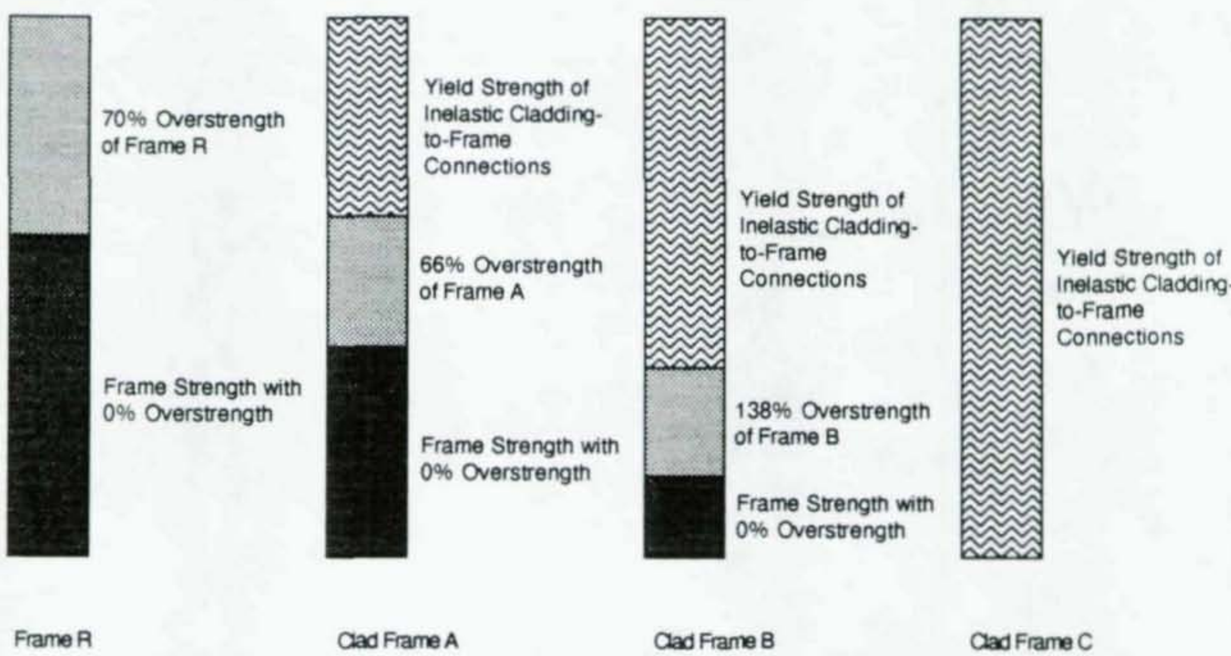

Fig. 2.4b Frame and Connection Strengths based on Frame R with 70% Overstrength

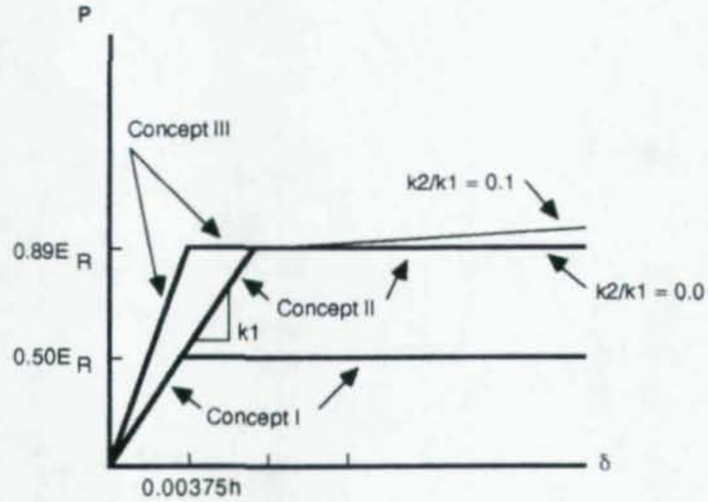

Fig. 2.5a Inelastic Top Panel Connections for Frame A

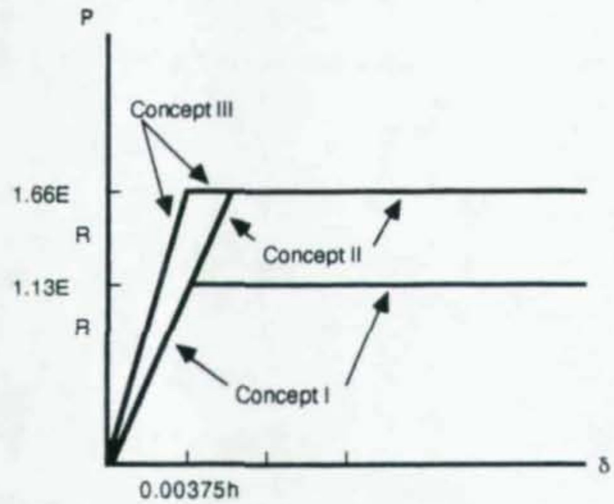

Fig. 2.5b Inelastic Top Panel Connections for Frame B

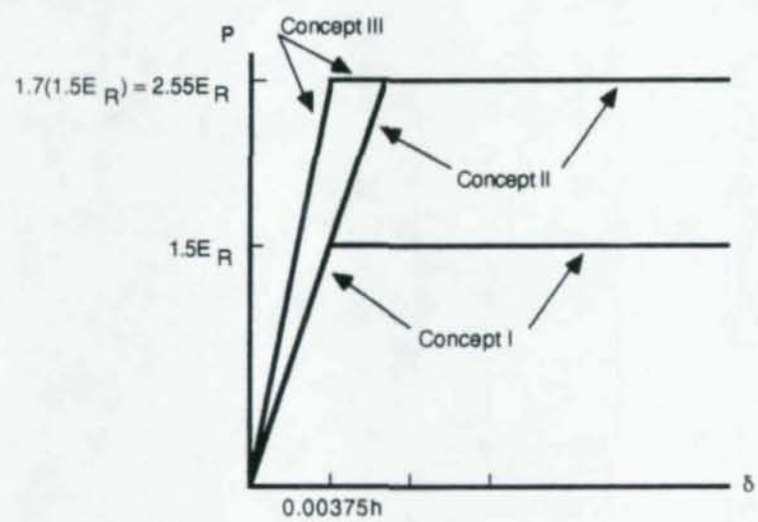

Fig. 2.5c Inelastic Top Panel Connections for Frame C

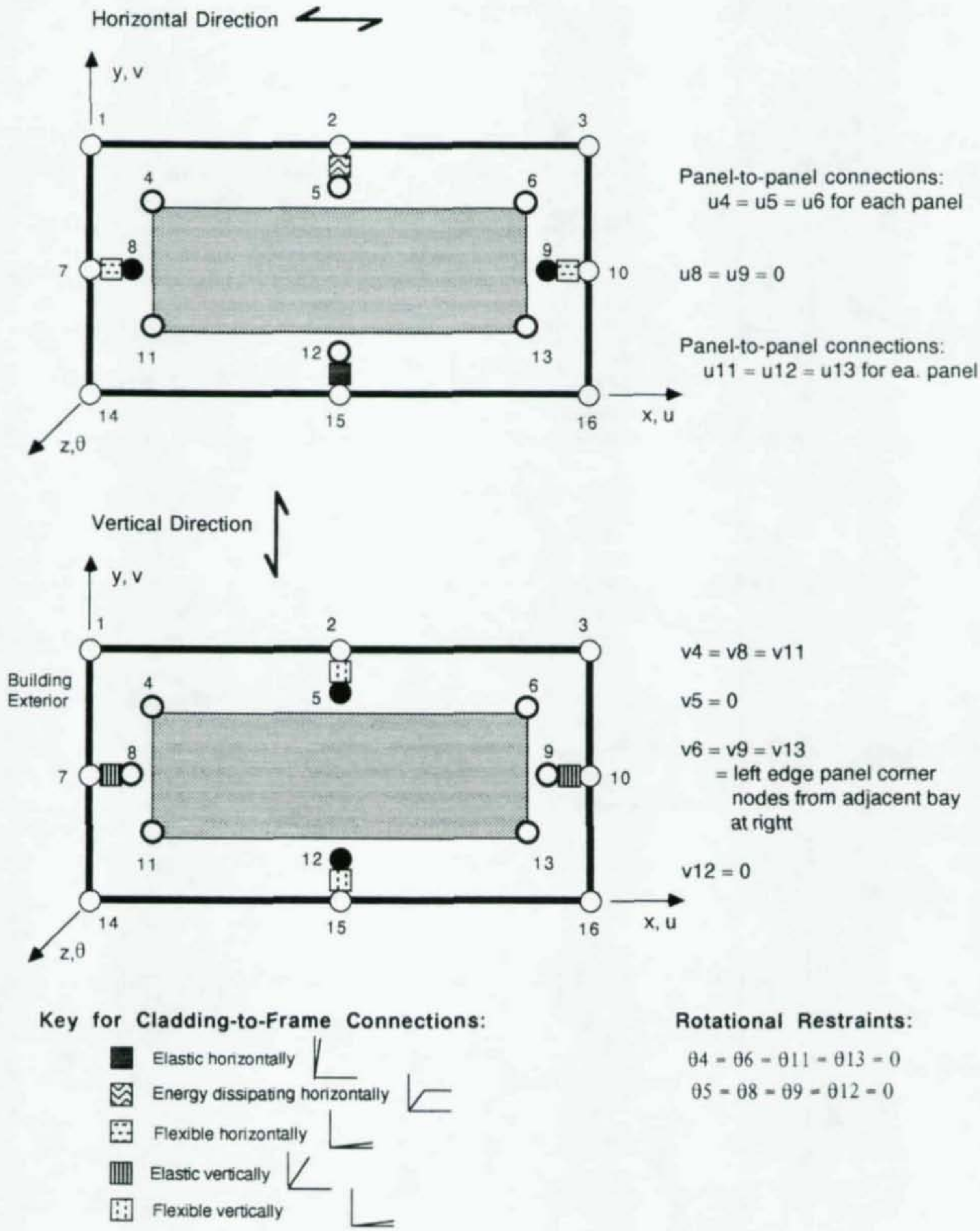

Fig. 3.1 Typical Bay: Restraint and Constraint of Nodes

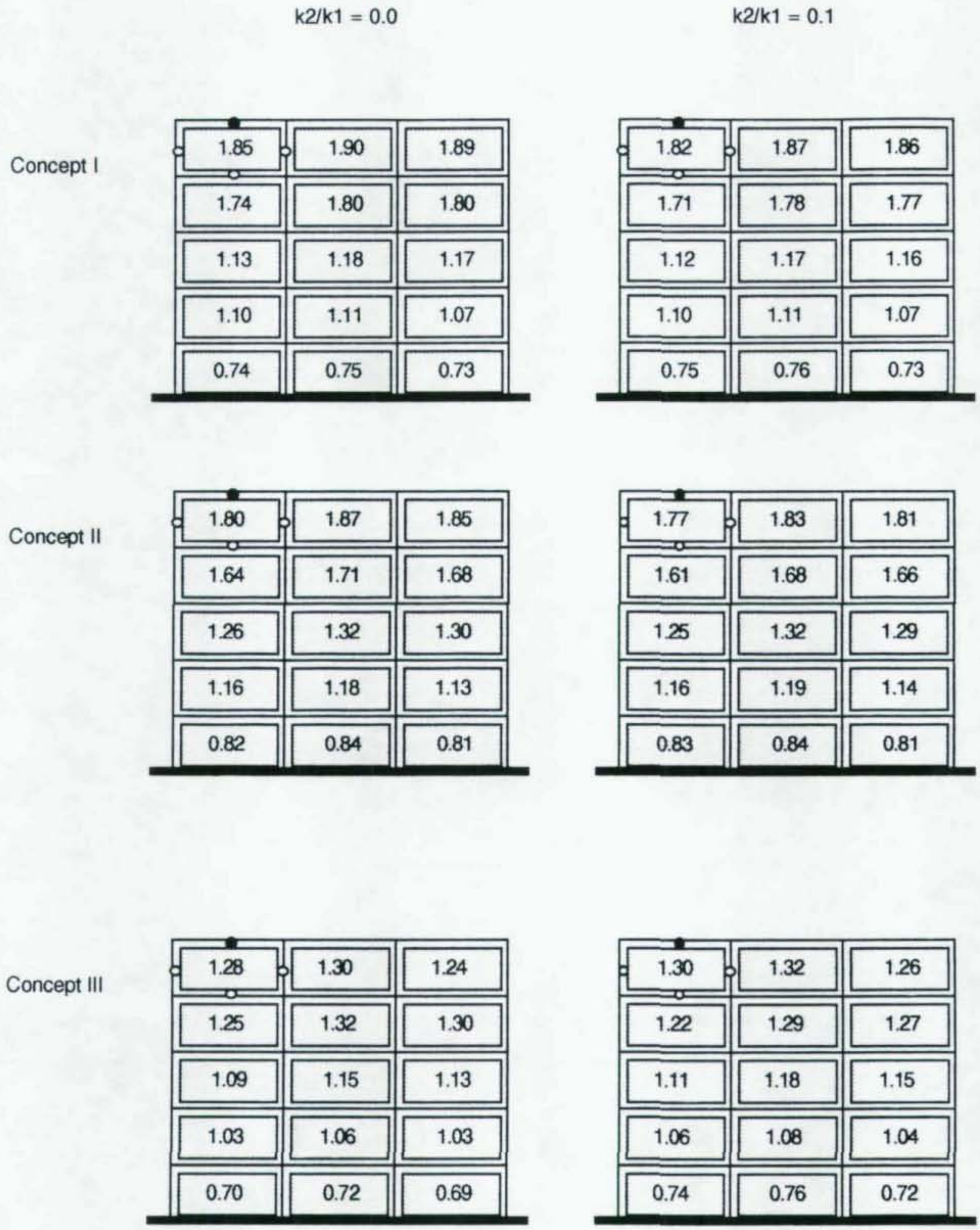

Fig. 4.1a Clad Frame A: Envelopes of Deformations (in.) of Top Panel Connections

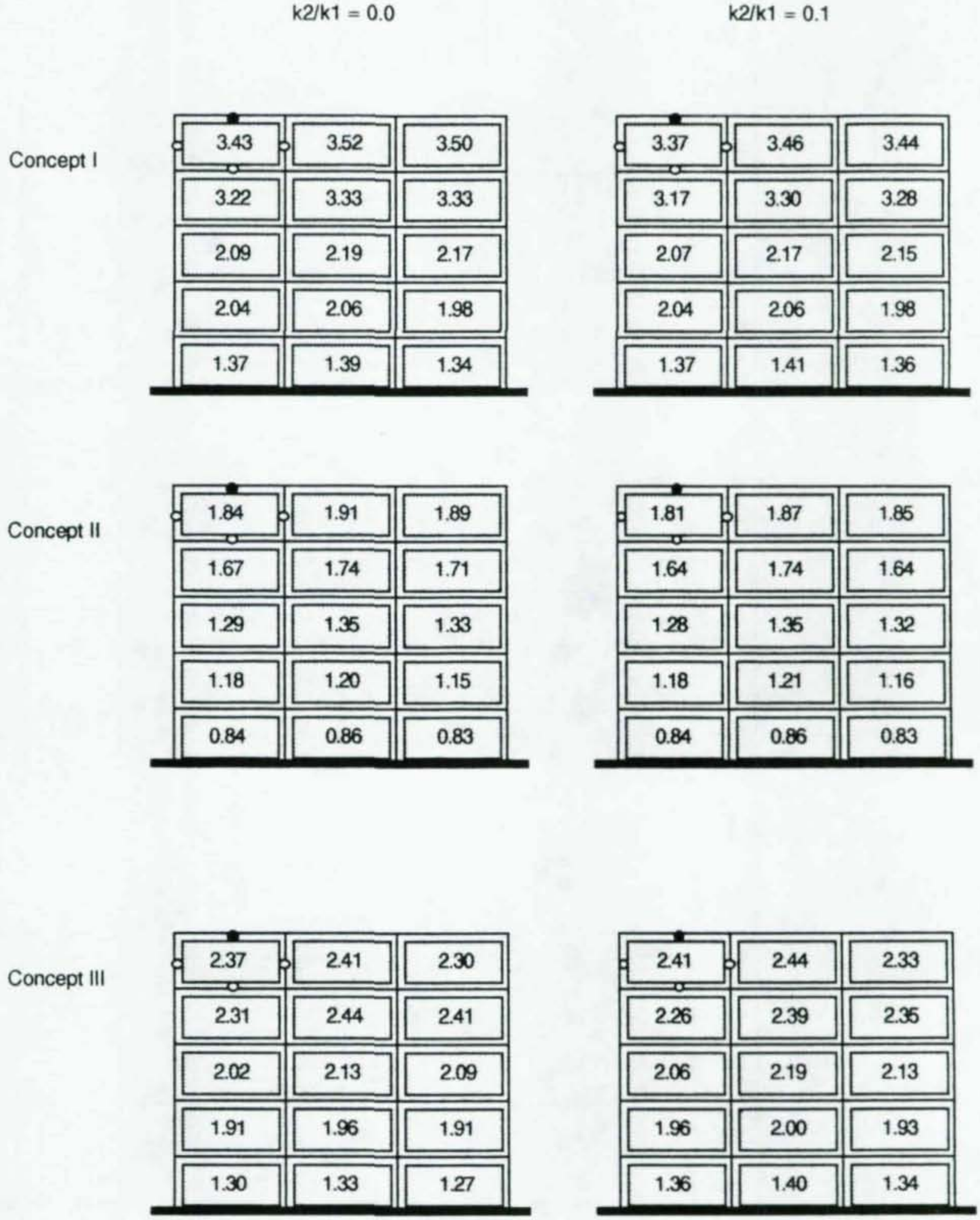

Fig. 4.1b Clad Frame A: Envelopes of Ductility Ratios for Top Panel Connections

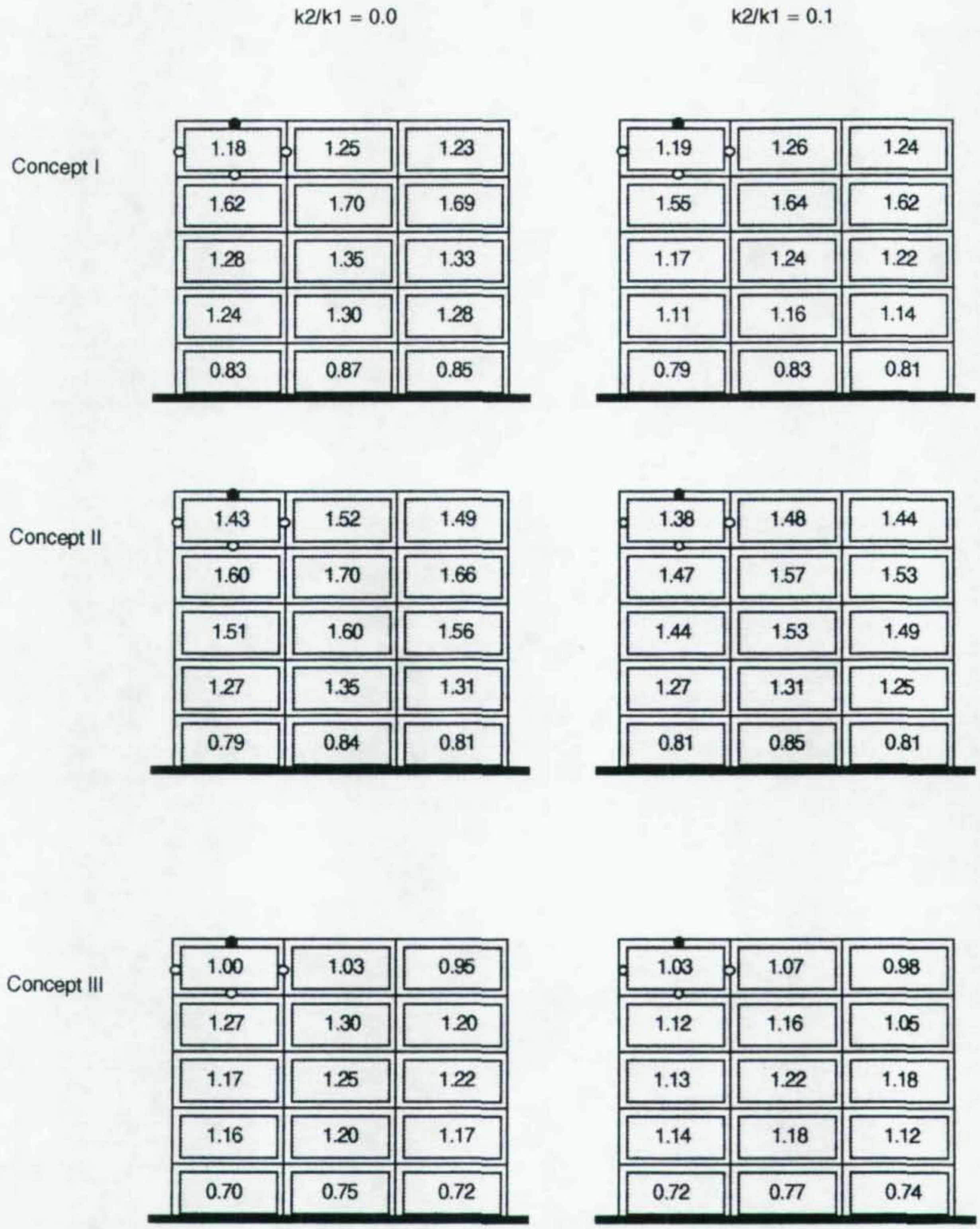

Fig. 4.2a Clad Frame B: Envelopes of Deformations (in.) of Top Panel Connections

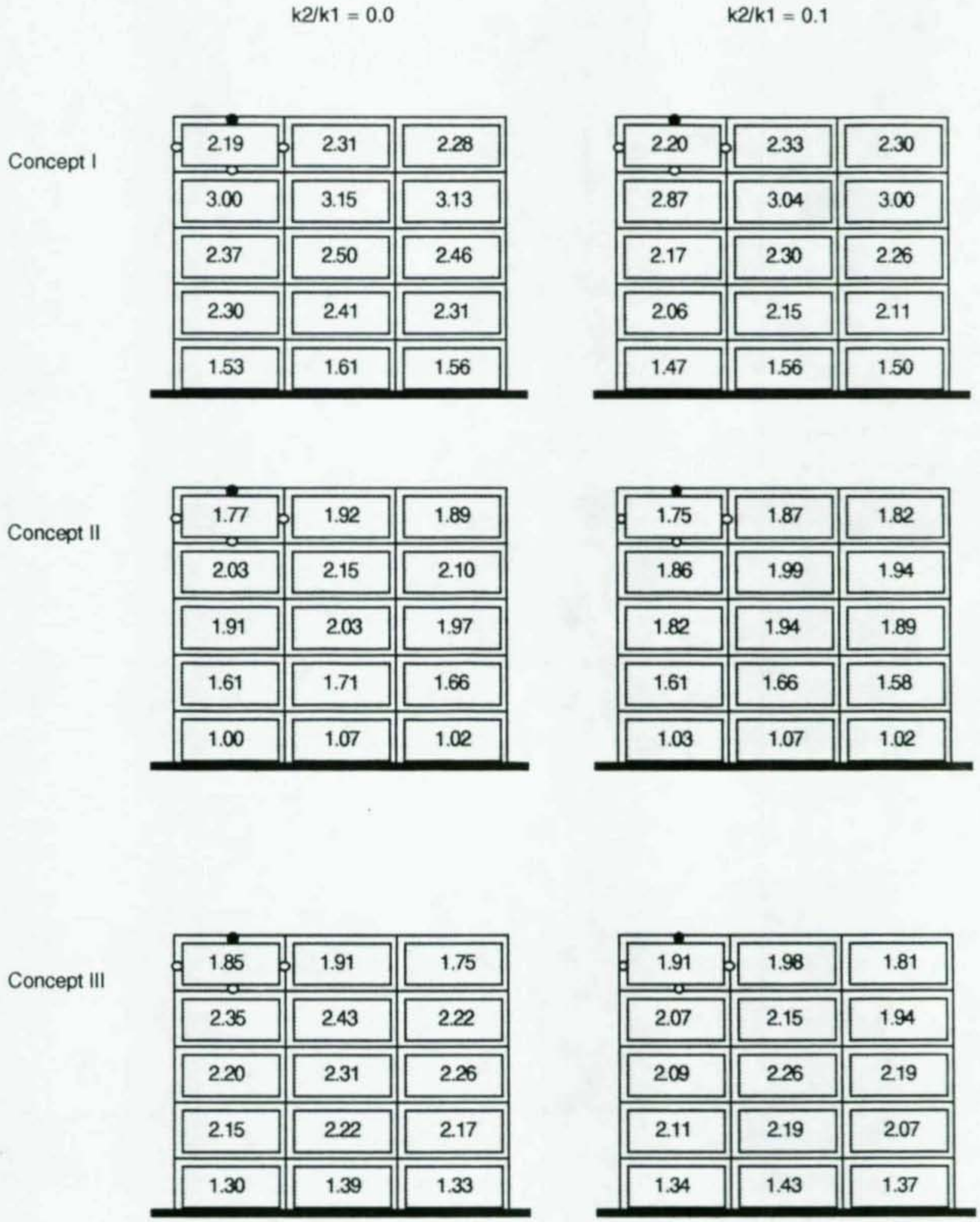

Fig. 4.2b Clad Frame B: Envelopes of Ductility Ratios for Top Panel Connections

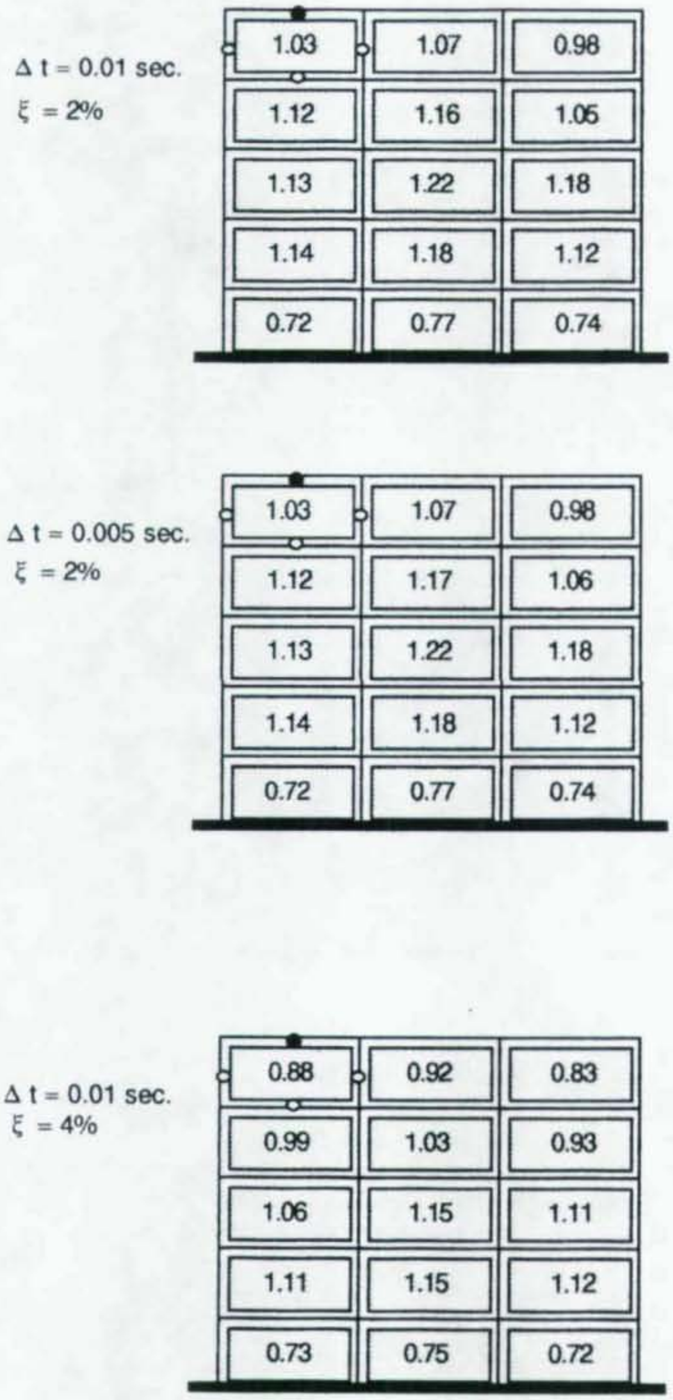

Fig. 4.3a **Clad Frame B, Concept III, k2/k1 = 0.1: Envelopes of Deformations (in.) of Top Panel Connections**

Δ t = 0.01 sec.
ξ = 2%

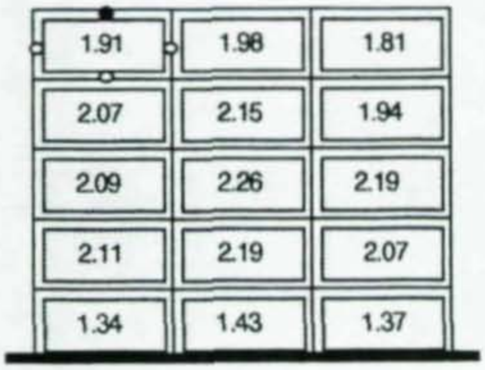

Δ t = 0.005 sec.
ξ = 2%

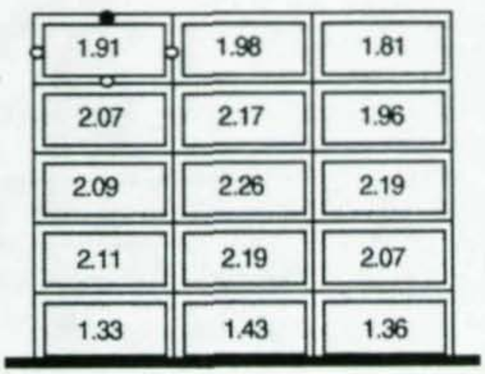

Δ t = 0.01 sec.
ξ = 4%

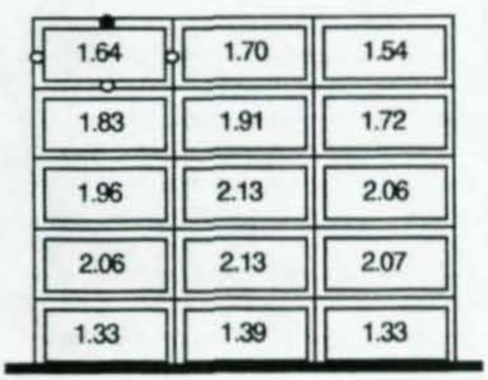

Fig. 4.3b Clad Frame B, Concept III, k2/k1 = 0.1: Envelopes of Ductility Ratios for Top Panel Connections

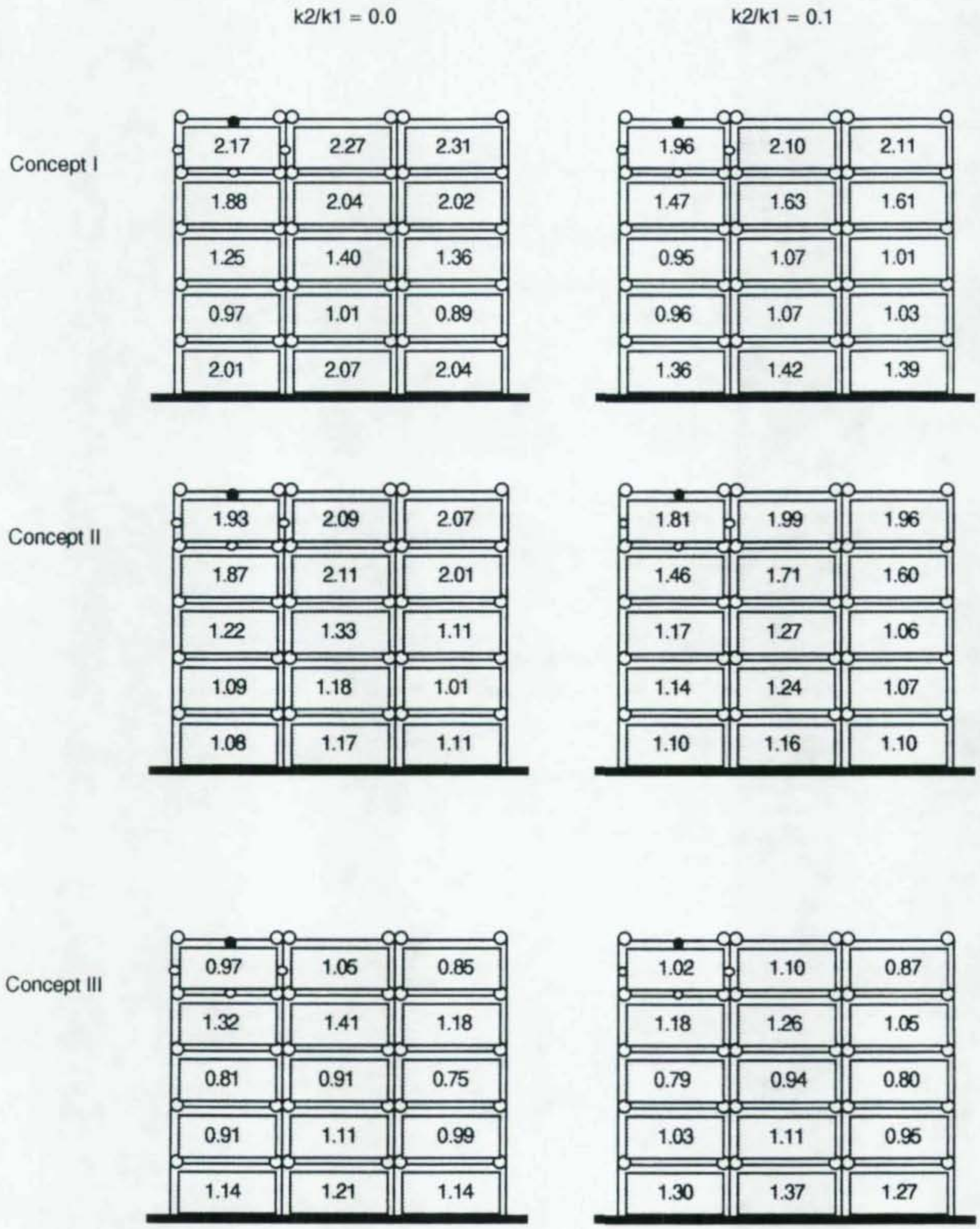

Fig. 4.4a Clad Frame C: Envelopes of Deformations (in.) of Top Panel Connections

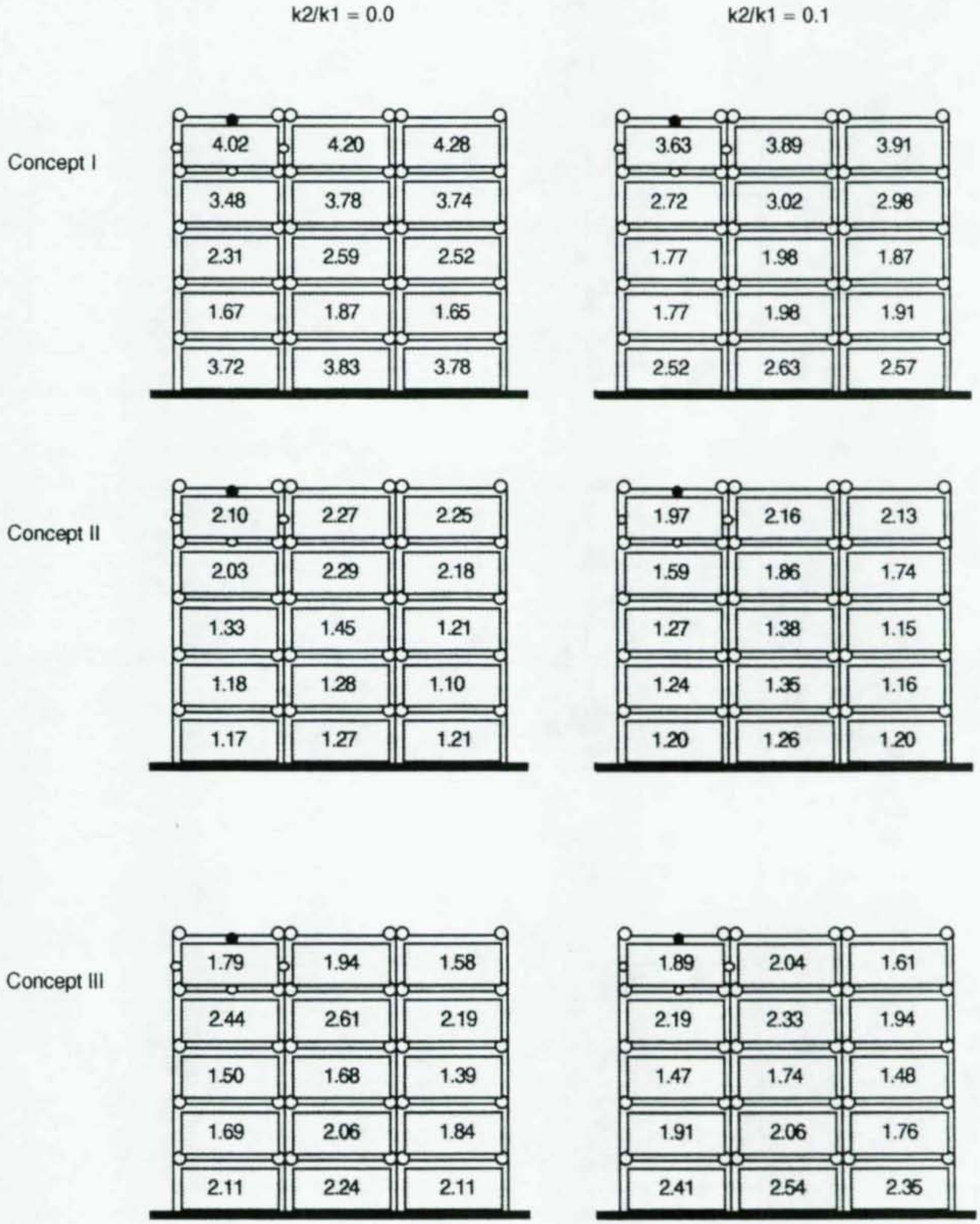

Fig. 4.4b Clad Frame C: Envelopes of Ductility Ratios for Top Panel Connections

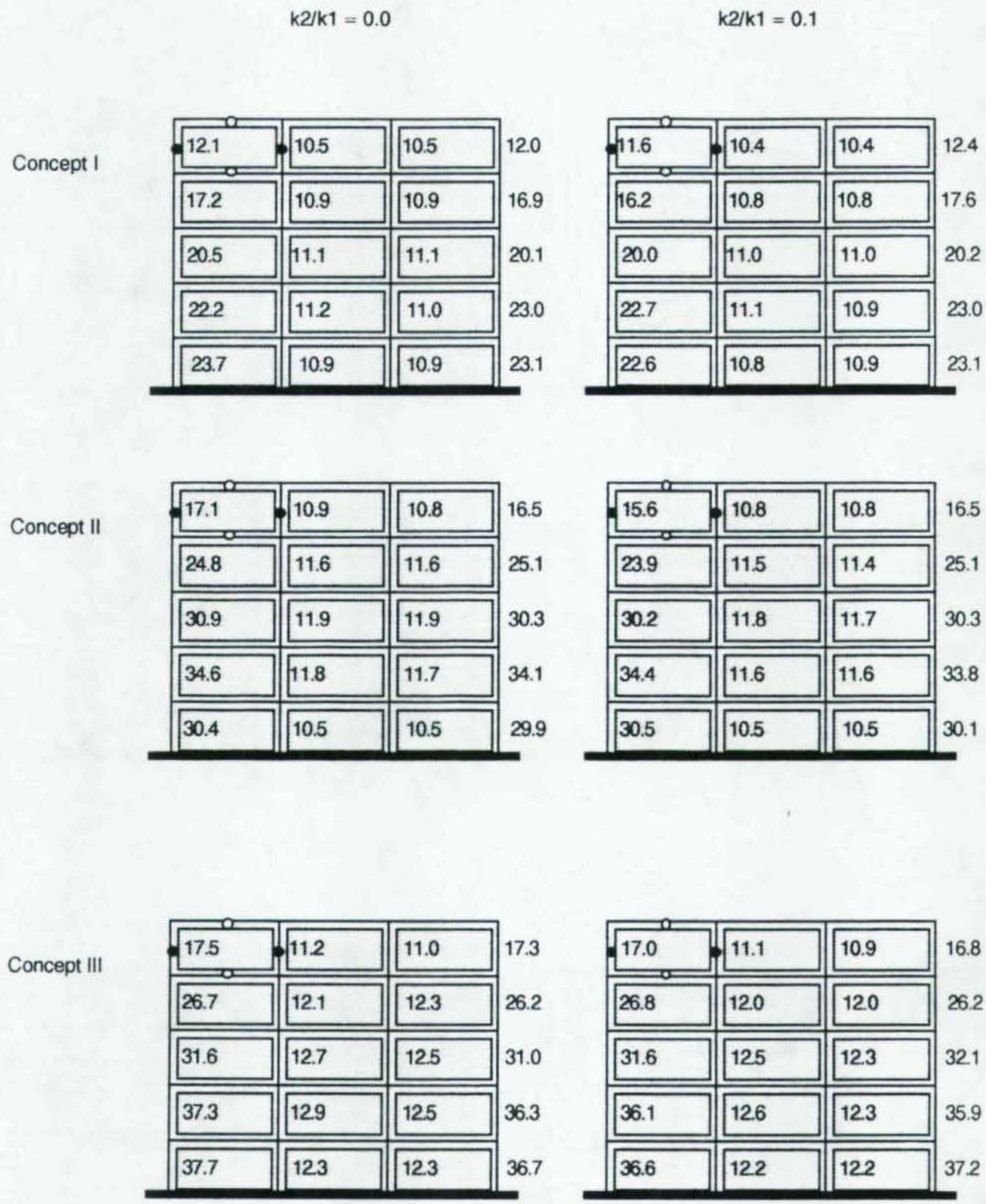

Fig. 4.5 Clad Frame A: Envelopes of Forces (kips) in Side Panel Connections

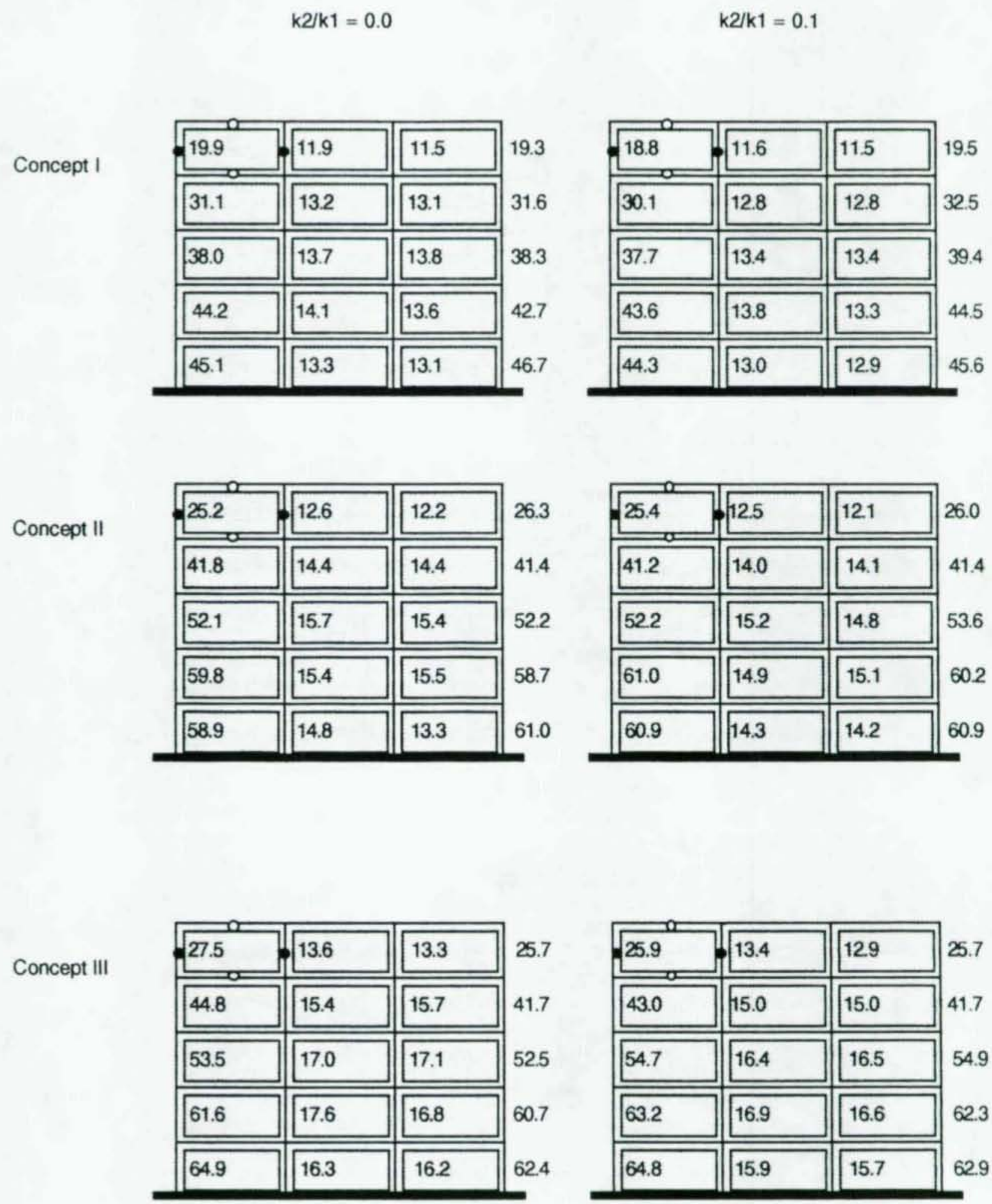

Fig. 4.6 Clad Frame B: Envelopes of Forces (kips) in Side Panel Connections

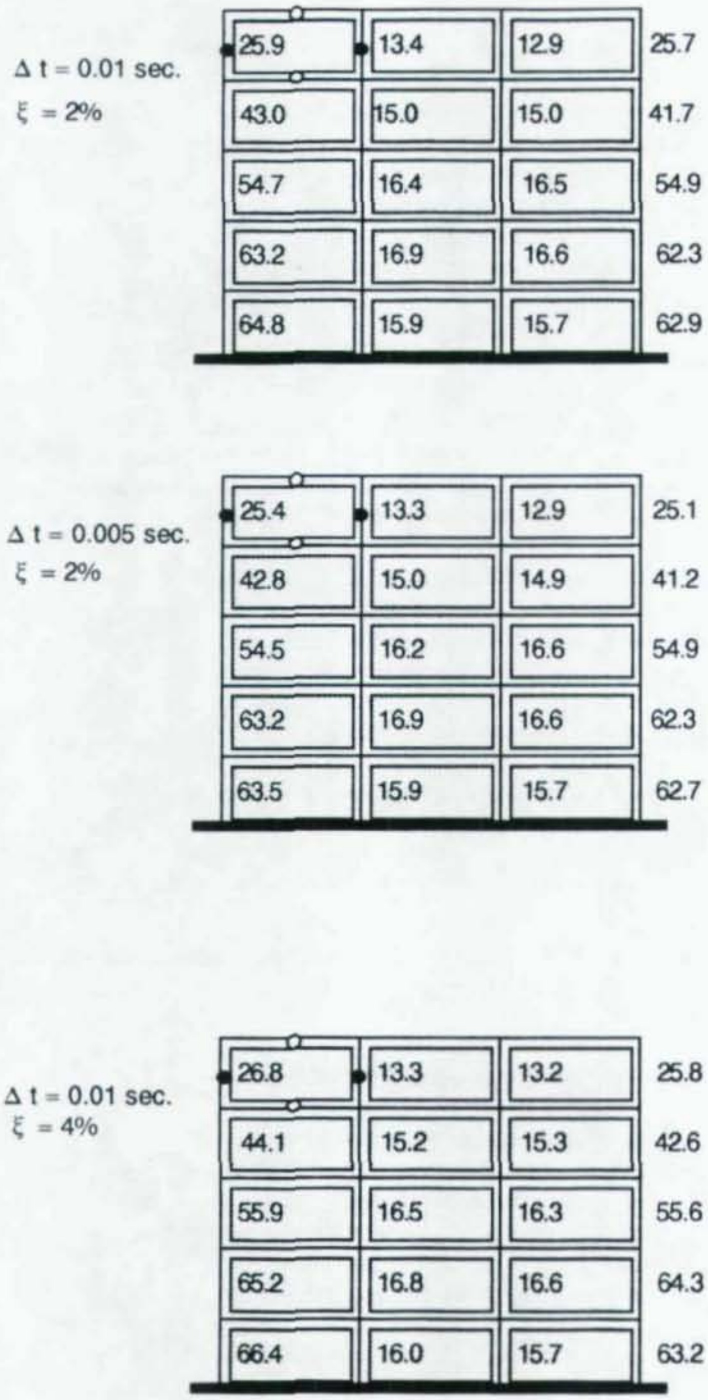

Fig. 4.7 Clad Frame B, Concept III, k2/k1 = 0.1: Envelopes of Forces (kips) in Side Panel Connections

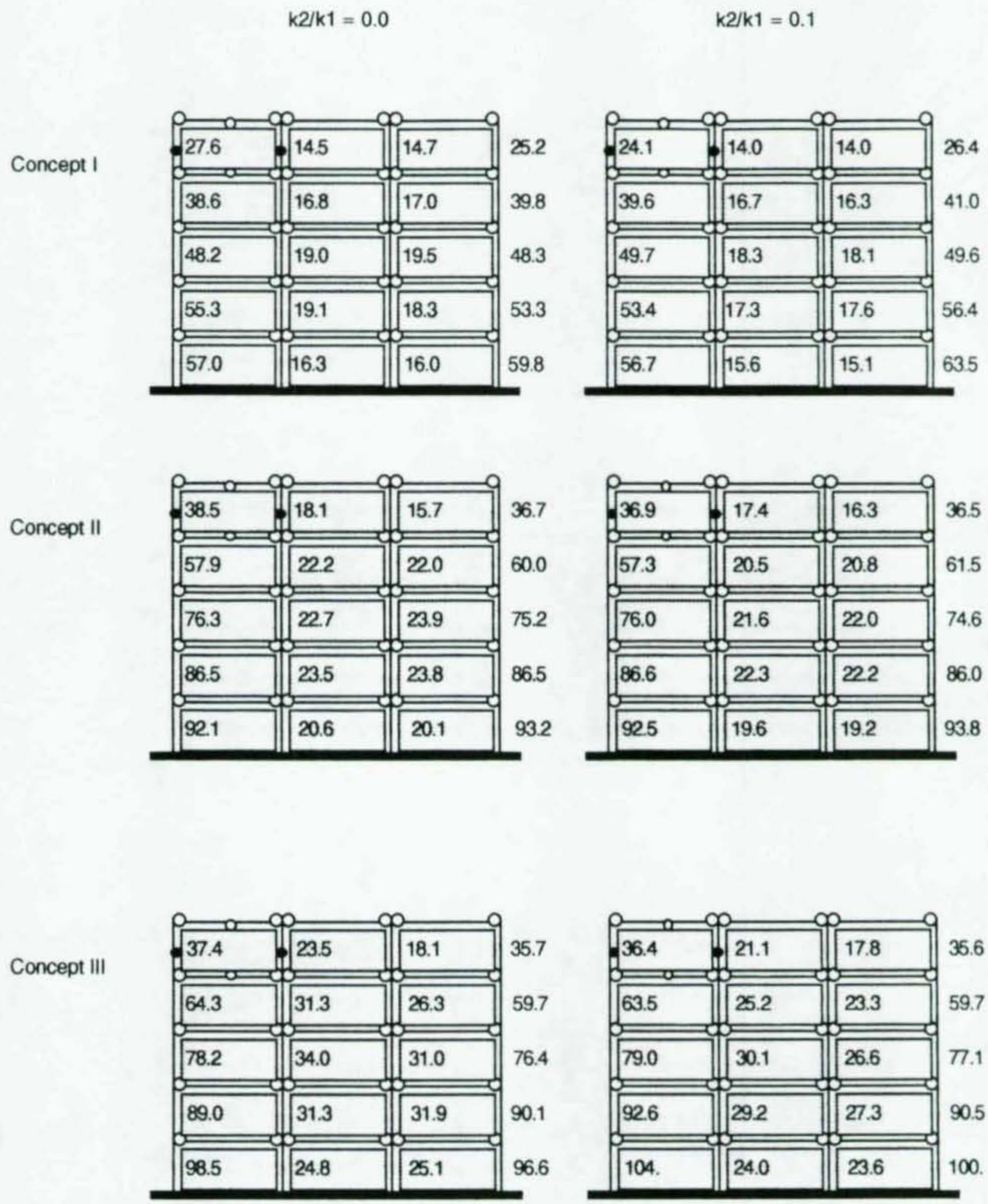

Fig. 4.8 Clad Frame C: Envelopes of Forces (kips) in Side Panel Connections

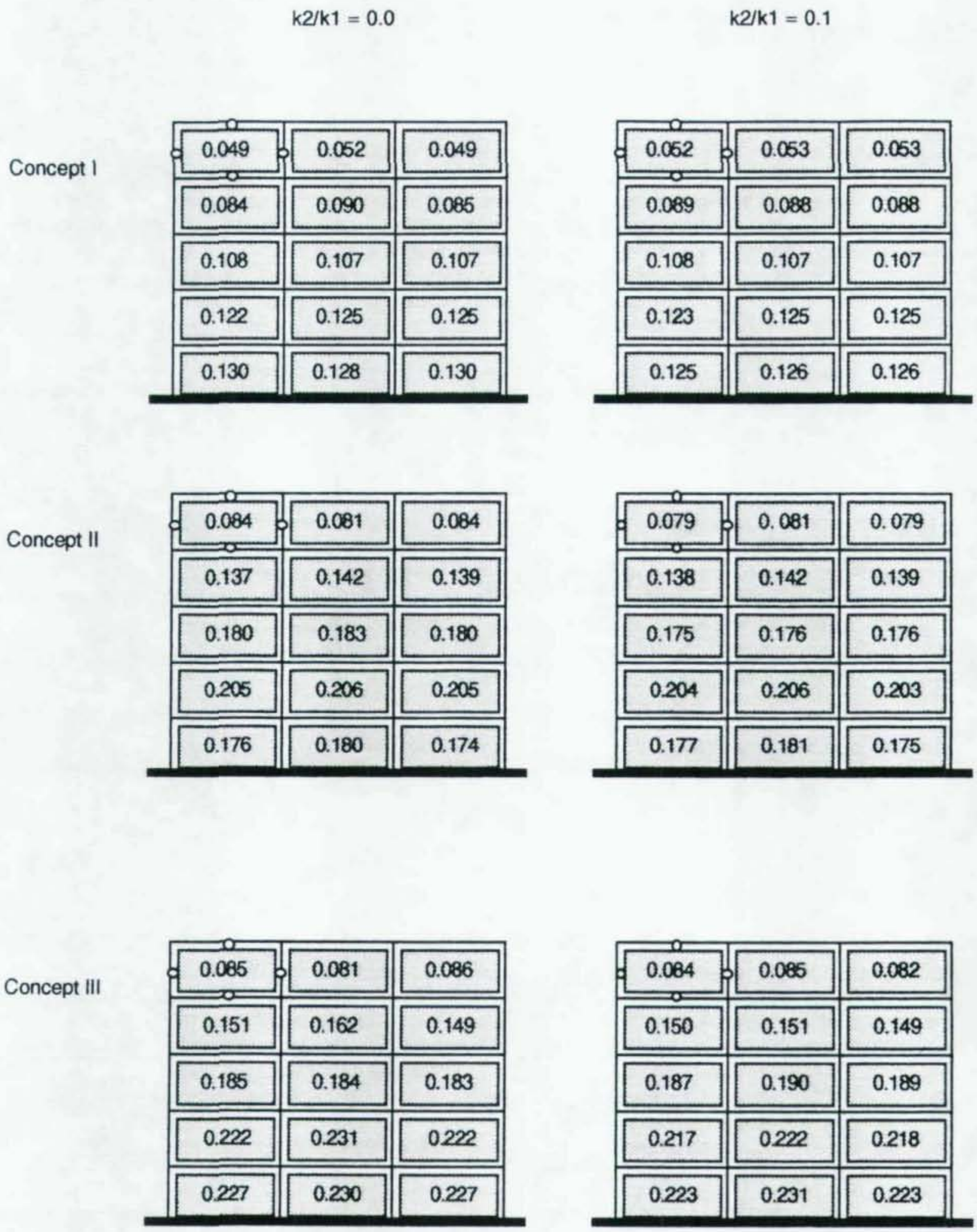

Fig. 4.9 Clad Frame A: Envelopes of Panel Shears (kip/in.)

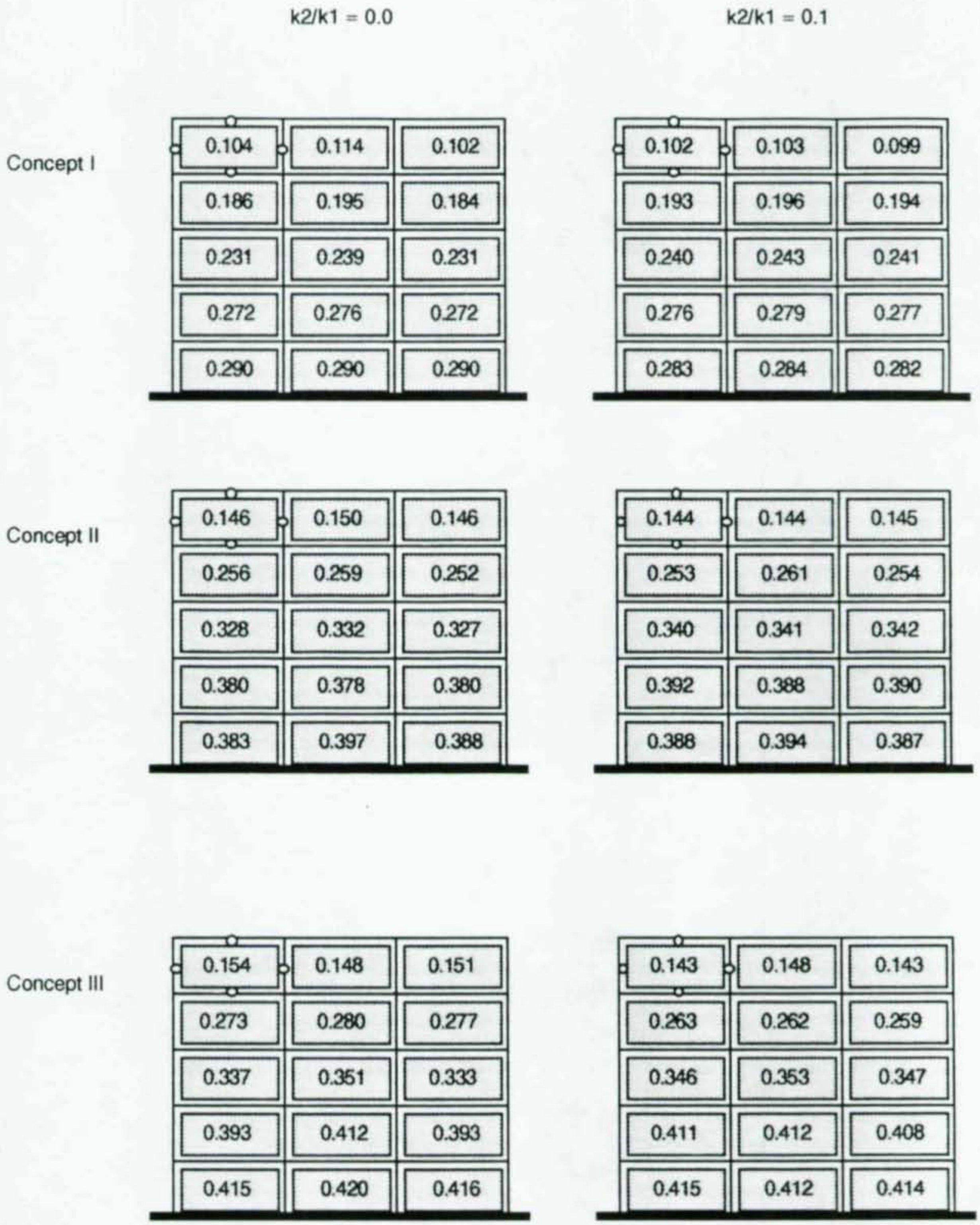

Fig. 4.10 Clad Frame B: Envelopes of Panel Shears (kip/in.)

Δ t = 0.01 sec.
ξ = 2%

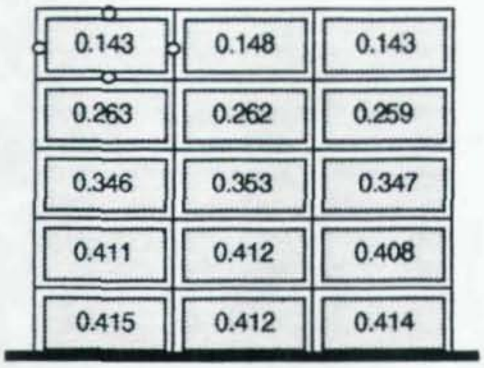

Δ t = 0.005 sec.
ξ = 2%

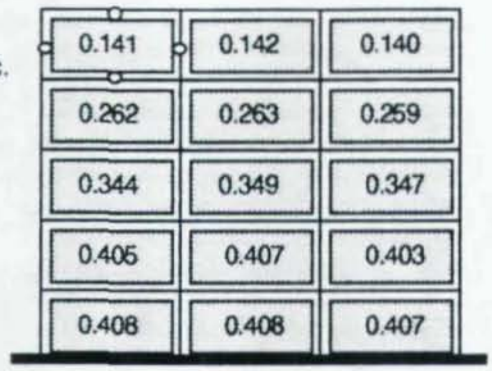

Δ t = 0.01 sec.
ξ = 4%

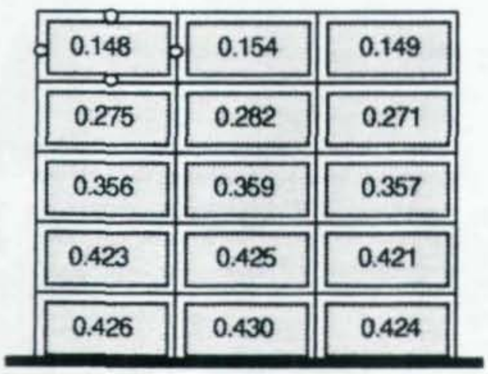

Fig. 4.11 Clad Frame B, Concept III, k2/k1 = 0.1: Envelopes of Panel Shears (kip/in.)

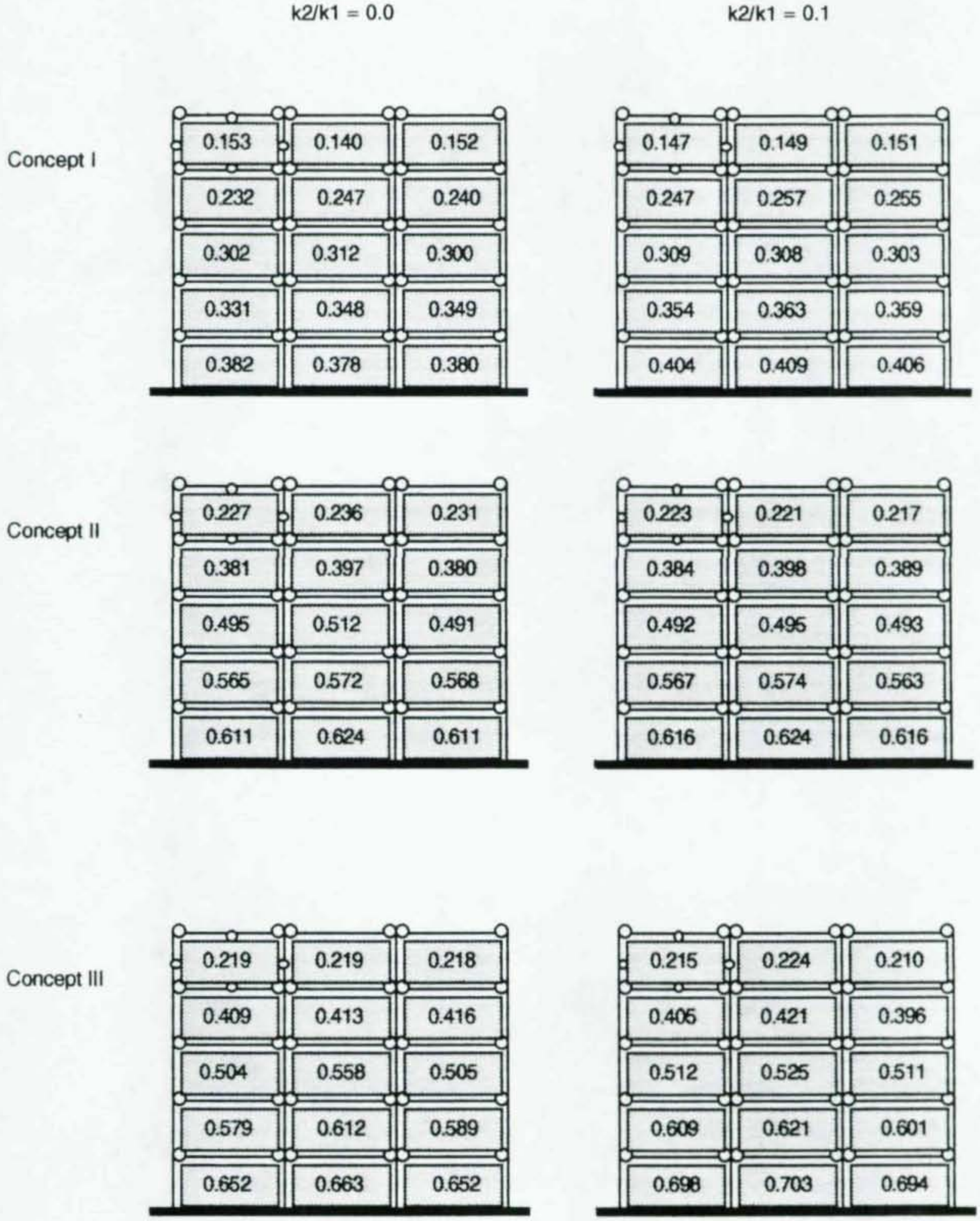

Fig. 4.12 Clad Frame C: Envelopes of Panel Shears (kip/in.)